Venting of a separate CO_2-rich gas phase from submarine arc volcanoes: Examples from the Mariana and Tonga-Kermadec arcs

John Lupton,[1] Marvin Lilley,[2] David Butterfield,[3] Leigh Evans,[4] Robert Embley,[1] Gary Massoth,[5,6] Bruce Christenson,[5] Ko-ichi Nakamura,[7] and Mark Schmidt[8]

[1]   Submersible dives on 22 active submarine volcanoes on the Mariana and Tonga-Kermadec arcs have discovered systems on six of these volcanoes that, in addition to discharging hot vent fluid, are also venting a separate CO_2-rich phase either in the form of gas bubbles or liquid CO_2 droplets. One of the most impressive is the Champagne vent site on NW Eifuku in the northern Mariana Arc, which is discharging cold droplets of liquid CO_2 at an estimated rate of 23 mol CO_2/s, about 0.1% of the global mid-ocean ridge (MOR) carbon flux. Three other Mariana Arc submarine volcanoes (NW Rota-1, Nikko, and Daikoku), and two volcanoes on the Tonga-Kermadec Arc (Giggenbach and Volcano-1) also have vent fields discharging CO_2-rich gas bubbles. The vent fluids at these volcanoes have very high CO_2 concentrations and elevated $C/^3He$ and $\delta^{13}C$ (CO_2) ratios compared to MOR systems, indicating a contribution to the carbon flux from subducted marine carbonates and organic material. Analysis of the CO_2 concentrations shows that most of the fluids are undersaturated with CO_2. This deviation from equilibrium would not be expected for pressure release degassing of an ascending fluid saturated with CO_2. Mechanisms to produce a separate CO_2-rich gas phase at the seafloor require direct injection of magmatic CO_2-rich gas. The ascending CO_2-rich gas could then partially dissolve into seawater circulating within the volcano edifice without reaching equilibrium. Alternatively, an ascending high-temperature, CO_2-rich aqueous fluid could boil to produce a CO_2-rich gas phase and a CO_2-depleted liquid. These findings indicate that carbon fluxes from submarine arcs may be higher than previously estimated, and that experiments to estimate carbon fluxes at submarine arc volcanoes are merited. Hydrothermal sites such as these with a separate gas phase are valuable natural laboratories for studying the effects of high CO_2 concentrations on marine ecosystems.

1. Introduction

[2]   Because magmas produced from melting of the mantle are typically CO_2-saturated at depths of at least several kilometers below the ocean floor, rising magma will inevitably lead to degassing [*Dixon et al.*, 1991; *Dixon*, 1997; *Wallace*, 2005]. Magmatic volatiles (H_2O, CO_2, SO_2, H_2S, H_2, He) that escape from rising magma are transported by hydrothermal fluids that may be sampled at seafloor vents. When the gas content of these vents is relatively low, the transfer of gas from magma to hydrothermal fluid may be considered as integrated with hydrothermal alteration in the reaction zone, i.e., that gases are extracted from whole rock. However, in many cases, the gas content of fluids exceeds what can be extracted from rock at physically reasonable water/rock ratios, and this requires that magmatic gas be injected into circulating hydrothermal fluids. It is absolutely clear that there is a large imprint of magmatic degassing in mid-ocean ridge systems such as Axial Volcano on the Juan de Fuca Ridge [*Butterfield et al.*, 1990], the East Pacific Rise at $9°50'N$ [*Lilley et al.*, 1992; *Von Damm et al.*, 1995; *Von Damm*, 1995], and the superfast spreading southern East Pacific Rise near $32°S$ [*Lupton et al.*, 1999]. Axial Volcano and the East Pacific Rise (EPR) $9°N$ sites are characterized by active magma chambers and recent

---

[1]Pacific Marine Environmental Laboratory, NOAA, Newport, Oregon, USA.
[2]School of Oceanography, University of Washington, Seattle, Washington, USA.
[3]JISAO, University of Washington, Seattle, Washington, USA.
[4]CIMRS, Oregon State University, Newport, Oregon, USA.
[5]Institute of Geological and Nuclear Sciences, Lower Hutt, New Zealand.
[6]Now at Mass-Ex3 Consulting LLC, Renton, Washington, USA.
[7]National Institute of Advanced Science and Technology, Tsukuba, Japan.
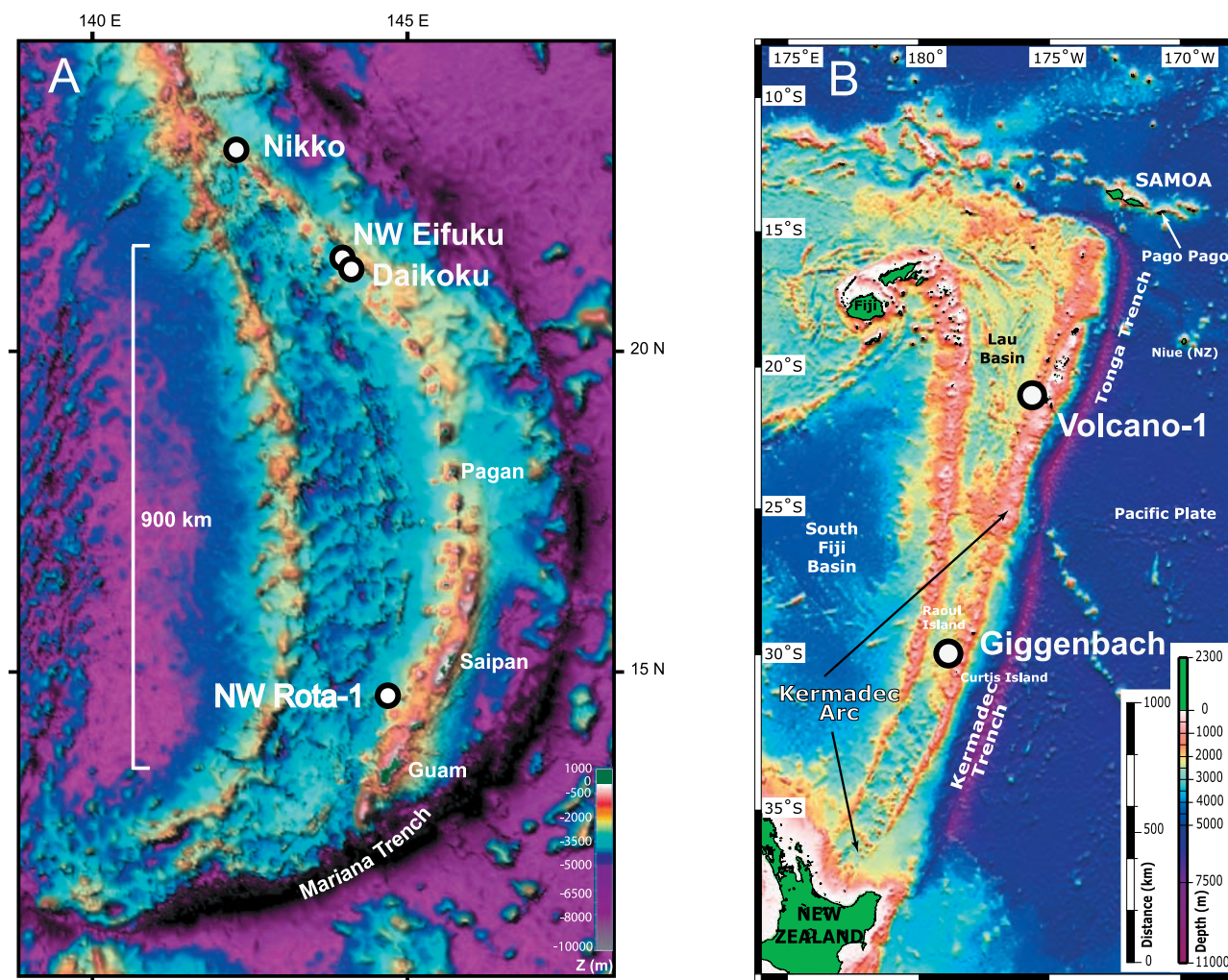[8]Institute of Geosciences, University of Kiel, Kiel, Germany.

Figure 1. Location map for submarine arc volcanoes venting a separate gas phase. (a) NW Rota-1, Daikoku, NW Eifuku, and Nikko on the Mariana Arc and (b) Giggenbach and Volcano-1 on the Tonga-Kermadec Arc.

eruptions. The pathways taken by exsolved magmatic volatiles may be complicated. By examining the manifestations of high gas content in hydrothermal systems, inferences can be made about the processes of degassing and gas transport to hydrothermal vents.

[3] Among the dozens of mid-ocean ridge (MOR) hydrothermal systems that have been studied over the past few decades, a significant discharge of gas bubbles has been found at only one site: the Magic Mountain vent field on the Explorer Ridge, northeast Pacific (D. Butterfield, private communication, 2007). In contrast to MOR systems, recent studies of submarine volcanoes on volcanic arcs have found several sites that, in addition to discharging hot vent fluid, are also venting a separate CO_2-rich phase either in the form of gas bubbles or liquid CO_2 droplets. These findings raise important questions as to the genesis of this separate gas phase and the relative contribution of degassing along volcanic arcs to the global carbon flux.

[4] In this paper we examine the hydrothermal systems on six submarine arc volcanoes that are venting a separate gas phase, with particular emphasis on the magmatic gases ^{3}He and CO_2. For each of these volcanoes the separate gas phase is composed of >90% CO_2. Four of these volcanoes are on the Mariana Arc: NW Eifuku, NW Rota-1, Nikko, and Daikoku (Figure 1a). In addition, we will discuss two other submarine volcanoes on the Tonga-Kermadec Arc, Giggenbach and Volcano-1, which are also venting CO_2-rich gas bubbles (Figure 1b).

2. Seagoing Expeditions

[5] Samples for this study were collected using both manned submersibles and remotely operated vehicles (ROVs) during five different expeditions. The initial exploratory work on the Mariana Arc was conducted in 2003 on the R/V *Thompson*, which completed bathymetric mapping and water column plume surveys of about 50 submarine volcanoes [*Embley et al.*, 2004]. This expedition found evidence for hydrothermal activity on about a dozen of these volcanoes, based on the existence of water column hydrothermal plumes [*Baker et al.*, 2008]. After this initial survey, follow-up expeditions in 2004, 2005, and 2006 completed submersible dives on 11 of these active Mariana Arc volcanoes (from south to north, these were Seamount X,

Forecast, NW Rota-1, Esmeralda, Ruby, East Diamante, Maug, Daikoku, NW Eifuku, Kasuga-2, and Nikko). With the exception of Esmeralda, the three expeditions were able to photograph and sample active vent sites on each of these Mariana Arc volcanoes. Surprisingly, of the 11 active volcanoes surveyed, four (NW Rota-1, Daikoku, NW Eifuku, and Nikko) (Figure 1a) were found to be venting a distinct gas phase either in the form of CO_2-rich gas bubbles or liquid CO_2 droplets. Specifically, samples were collected with the ROV ROPOS during Cruise TN167 of the R/V *Thompson* in March–April 2004, with the ROV Hyper-Dolphin during Cruise NT05–18 aboard the Japanese ship R/V *Natsushima* in October–November 2005, and with the ROV Jason 2 during Cruise MGLN02MV of the R/V *Melville* in April–May 2006 [*Merle et al.*, 2004, 2006; *Nakamura*, 2005]. The R/V *Thompson* and R/V *Melville* expeditions were part of the Submarine Ring of Fire (SRoF) project funded by NOAA's Office of Ocean Exploration.

[6] For the submarine volcanoes of the Tonga-Kermadec Arc, much of the water column exploratory work was conducted in a series of expeditions involving collaboration between New Zealand, Australian, and U.S. scientists [*de Ronde et al.*, 2001, 2007; *Massoth et al.*, 2003, 2007]. On the basis of these findings, in April–May 2005 the New Zealand–American Submarine Ring of Fire Project, supported by the New Zealand government and by NOAA's office of Ocean Exploration, conducted a series of *Pisces* submersible dives from the support ship R/V *Ka'imikai-o-Kanaloa* (KOK) [*Merle et al.*, 2005]. This work focused on eight submarine volcanoes thought to be hydrothermally active (from south to north these were Clark, Rumble V, Healy, Brothers, Volcano-W, Macauley, Giggenbach, and Monowai). As an extension of this project, in June of 2005 the German Submersible Investigations of the Tonga-Kermadec Arc using Pisces (SITKAP) expedition conducted additional *Pisces* dives on three volcanoes located farther north: Volcano-19, Volcano-18s, and Volcano-1 [*Stoffers et al.*, 2005]. Out of the total of 11 active volcanoes surveyed along the Tonga-Kermadec Arc, two (Giggenbach and Volcano-1) were found to be venting CO_2-rich gas bubbles (Figure 1b).

3. Methods

[7] Vent fluid samples were collected using special titanium alloy gas-tight bottles having an internal volume of $\sim$150 cm^3. Each bottle was pumped to a high-vacuum prior to each submersible dive. In most cases the gas-tight bottles were fitted with a short piece of Peek™ tubing connecting to a Ti sampling snout which was inserted into the vent orifice. The Peek™ tubing as well as the internal dead volume of the gas-tight bottle itself was filled with deep seawater prior to the dive to displace air and other gases. After the sampling snout was inserted into the vent orifice, the submersible triggered the bottle by depressing the rod on the trigger cylinder. This opened the inlet valve to the gas-tight bottle, and the hydraulic pressure at depth forced the sample into the evacuated volume, usually within a fraction of a second. After the sampling was completed, the trigger cylinder was released, sealing the sample in the bottle.

[8] After each dive the samples were processed on a seagoing high vacuum line. The gas-tight bottle, containing the sample consisting of a mixture of fluid and gas, was connected to the vacuum line and all connecting lines were evacuated using a combination of a mechanical pump and an oil diffusion pump. After sufficient vacuum was achieved, the line was placed in static condition, and the sample consisting of a mixture of fluid and gas was dropped into an evacuated flask. Sulfamic acid powder was added to the flask previous to the extraction in order to acidify the sample and aid in the release of dissolved CO_2. The water in the flask was then agitated with an ultrasonic cleaner, and as the gases were released a metal bellows pump was used to pump the gases through a chilled U-trap ($-60°C$) into a calibrated volume. The U-trap removed the water vapor so that only dry gas reached the calibrated volume. After about 10 min, over 90% of the dissolved gases were released, and then the pressure in the calibrated volume was measured at a known temperature with a precision capacitance manometer. Multiple splits of the extracted gases were then sealed into glass ampoules. For general gas analysis Pyrex ampoules were used, while samples for helium and rare gas analysis were sealed into ampoules constructed of alumino-silicate glass with low helium permeability. With this method there was no need to poison the samples since the gas was dry and no microbes were in contact with the extracted gases. At the end of the extraction, the water frozen in the U-trap was melted and then combined with the water remaining in the extraction flask. The water was then weighed to determine the total sample weight and then saved in Nalgene bottles for subsequent analysis of Mg and other fluid properties.

[9] In contrast to the sampling of vent fluids, the collection of gas bubbles and liquid CO_2 droplets presented a special challenge. As described previously [*Lupton et al.*, 2006], sampling the liquid CO_2 at NW Eifuku was particularly difficult because the liquid CO_2 expanded by a factor of $\sim$1000 when converted to CO_2 gas at 1 atm pressure. Furthermore, the liquid droplets tended to stick together like clusters of grapes rather than coalescing into a single large droplet. Therefore, at NW Eifuku, a special "droplet catcher" was used in combination with a small volume ($\sim$10 cm^3) Ti gas-tight bottle [*Lupton et al.*, 2006] (Figure 2a). After the coil spring of the droplet catcher was filled with CO_2 droplets, the spring was compressed thereby expelling most of the water while retaining the droplets. This resulted in a much higher concentration of the droplets being drawn into the gas-tight bottle. For the collection of gas bubbles at Giggenbach and Volcano-1 with the *Pisces* submersible, a plastic cylinder normally used for sediment sampling was modified by attaching a relief valve (Figure 2b). The submersible then completely filled the cylinder with the gas bubbles and closed the large ball valve integral to the cylinder. As the submersible ascended and hydrostatic pressure was released, the excess gas was allowed to escape through the relief valve. Because there is no water in the sample, minimal fractionation is expected during this gas loss. At the end of the dive, the gas sample was transferred from the plastic cylinder into a stopcock flask constructed of alumino-silicate glass or drawn into one of the Ti gas-tight bottles. The gas samples from the Mariana Arc volcanoes were
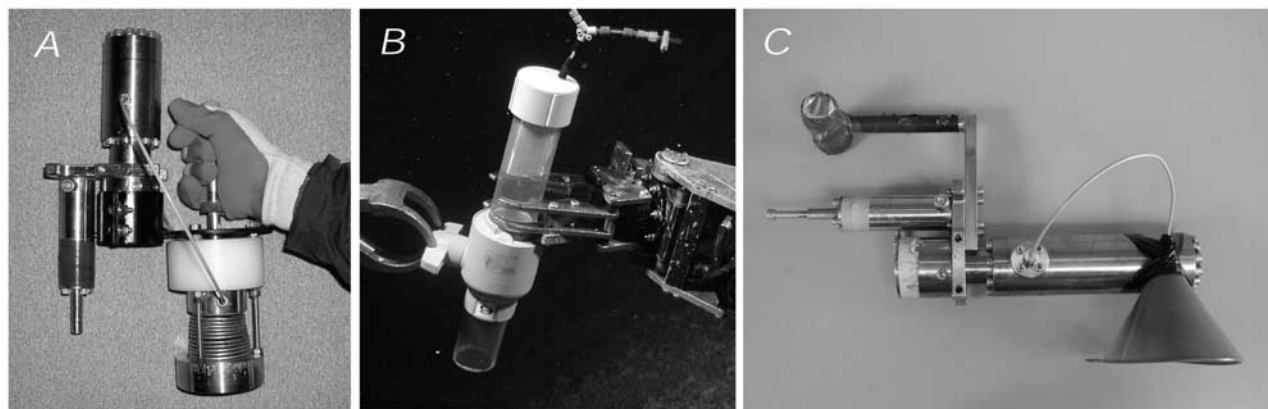
Figure 2. Photographs of methods used to collect gas phase samples. (a) Coil spring droplet catcher attached to the small volume (10 cm^3) Ti gas-tight bottle. This apparatus was used to collect liquid CO$_2$ droplets at the Champagne site, NW Eifuku. (b) Plastic cylinder fitted with a relief valve used for gas collections from the *Pisces* submersible. (c) Plastic funnel attached to 150 cm^3 gas-tight bottle.

sampled using a plastic funnel attached to one of the Ti gas-tight bottles with a short length of Peek™ tubing (Figure 2c). The ROV simply held the inverted funnel over the stream of rising gas bubbles, and then triggered the gas-tight bottle after the funnel was filled with gas. The gas samples were processed on the seagoing vacuum line in the same manner as described above for the vent fluid samples, with the exception that the sulfamic acid and ultrasonic agitation were omitted.

[10] Helium and neon concentrations and helium isotope ratios were determined using a special 21-cm radius mass spectrometer at the Helium Isotope Laboratory, Newport, Oregon. CO$_2$, CH$_4$, H$_2$ and other gas concentrations were determined by gas chromatography at three different laboratories: at the University of Washington, at the Institute of Geological and Nuclear Sciences, New Zealand, or at the Institute of Geosciences, University of Kiel, Germany. Carbon isotope ratios were determined by mass spectrometry at the University of Washington and at the University of Otago, New Zealand.

4. The Volcanoes

4.1. NW Rota-1

[11] NW Rota-1, located at 14.60°N, 144.77°E on the southern Mariana Arc, is a steep-sided basaltic and basaltic-andesite cone that rises to a depth of 517 m at its summit [*Embley et al.*, 2006; *Chadwick et al.*, 2008] (Figure 3a). A robust water column plume was present over the volcano summit in 2003, 2004, and 2006, suggesting that hydrothermal activity was continuous over this entire period (J. Resing, private communication, 2007). NW Rota-1 was first sampled in 2004 with a series of dives of the Canadian submersible ROPOS. At about 540 m depth on the volcano, ROPOS discovered a crater, later named Brimstone Pit, that was actively erupting volcaniclastic material into a pulsating, acidic plume (pH 2.0, 25°C) laden with particulate sulfur (Figure 4a) [*Embley et al.*, 2006]. In addition to the pit crater, several additional active vents were found at depths between 530 and 590 m on the volcano summit venting clear CO$_2$-rich fluid at temperatures up to 62°C (Table 1). The volcano was visited again in 2005 with the

Hyper-Dolphin ROV, but no gas samples were taken. The Hyper-Dolphin dives in 2005 found that the Brimstone Pit was still actively erupting and had formed a cinder cone and grown upward by about 20 m [*Embley et al.*, 2006; *Chadwick et al.*, 2008]. When the volcano was visited next with Jason 2 in 2006, it had changed considerably. The cinder cone observed in 2005 was gone, and the Brimstone Pit eruptive vent was now about 30 m deeper. Furthermore, as detailed by *Chadwick et al.* [2008], the eruptive vent had entered an extremely active phase characterized by expulsion of red-glowing rock, intense turbidity plumes, and venting of a gas and/or steam phase (Figure 4b).

[12] In 2004 and 2006 several good samples of the Brimstone Pit fluid ranging between 25 and 120°C were collected with the Ti gas-tight bottles. The fluid was quite remarkable in having high acidity (pH 2.0) and high CO$_2$ content (up to 80 mmol/kg) despite its moderate temperature. In addition to numerous vent fluid collections, on dives J2−188 and J2−189 in 2006, two excellent samples of the Brimstone Pit gas phase were collected using an inverted funnel in combination with one of the gas-tight bottles. As shown in Table 1, this gas was composed of 90% CO$_2$, 10% H$_2$, with trace amounts of CH$_4$. It is also notable that this gas composition was reproducible from collections on two separate dives on consecutive days.

4.2. Daikoku

[13] Daikoku, located at 21.32°N, 114.19°E, is a large cone that rises to a summit depth of ∼350 m (Figure 3b). It has a 200 m diameter summit crater that contains two very deep pit craters [*Embley*, 2006; *Embley et al.*, 2007]. ROV dives on Daikoku in 2004 and 2005 found diffuse venting at temperatures of 15 to 17°C. No fluid samples were collected in 2004, and in 2005 only a pair of diluted gas-tight bottle samples were collected from the Bottomless Pit with the Hyper-Dolphin (Table 1).

[14] In 2006 the Jason 2 dives on Daikoku explored a deeper area of the volcano to the northwest of the summit [*Merle et al.*, 2006]. These 2006 dives discovered a series of new active vents including an impressive pond of liquid sulfur with a measured temperature of 187°C. This pond, named Sulfur Cauldron, had a crust on its surface formed by
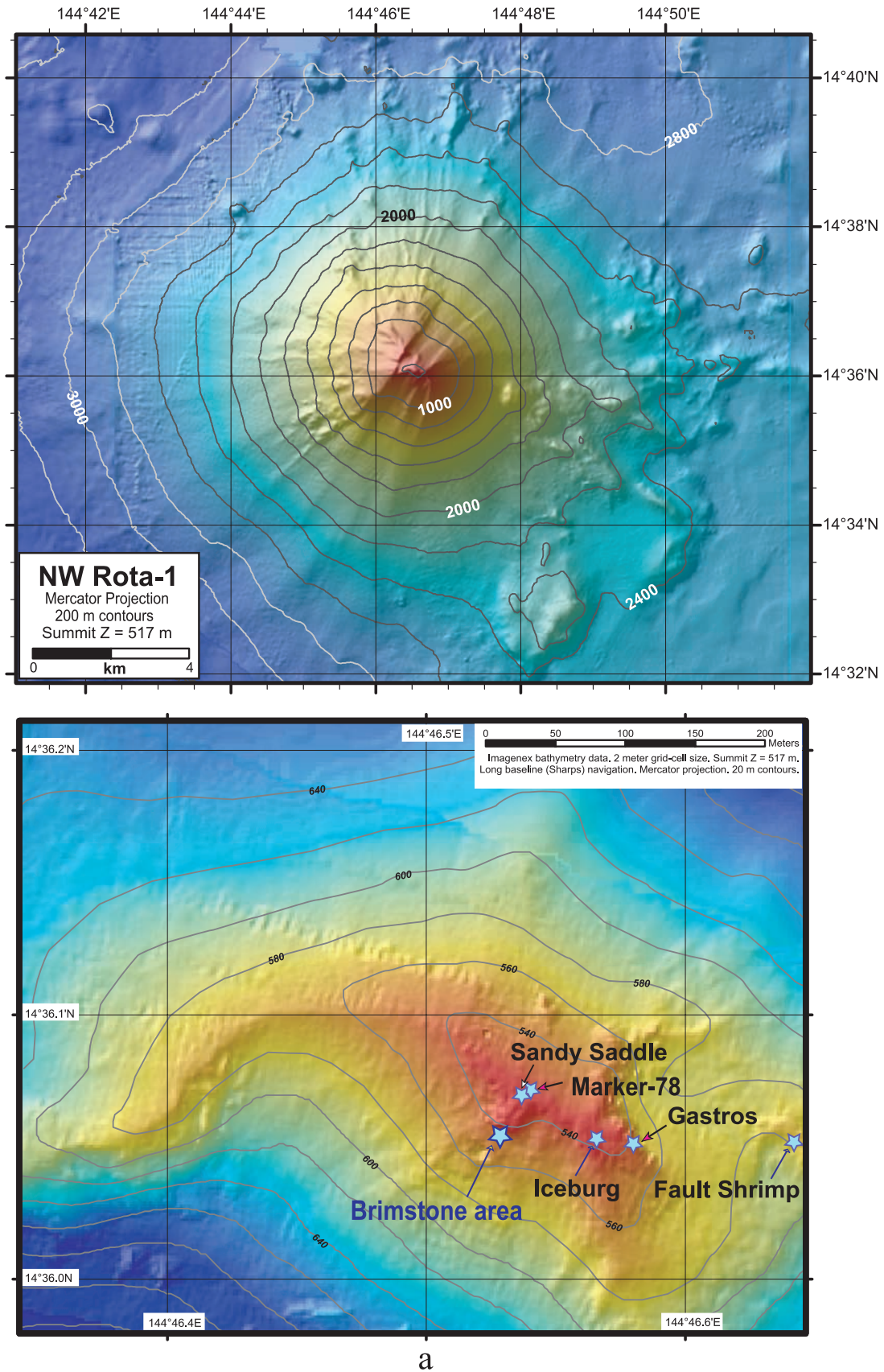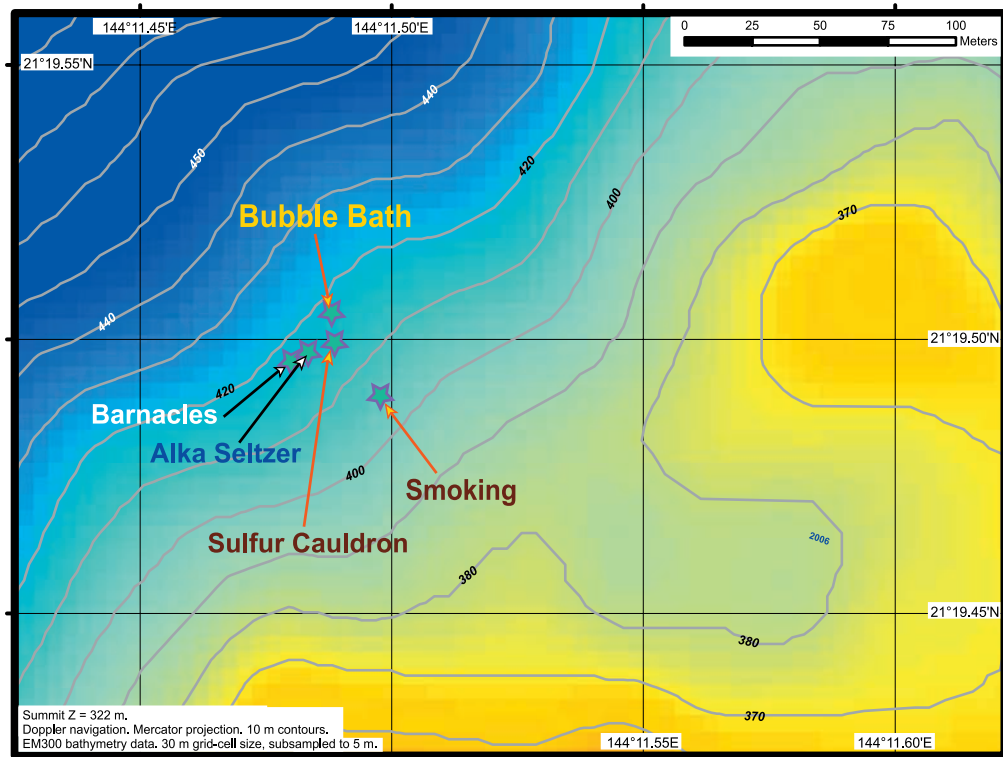
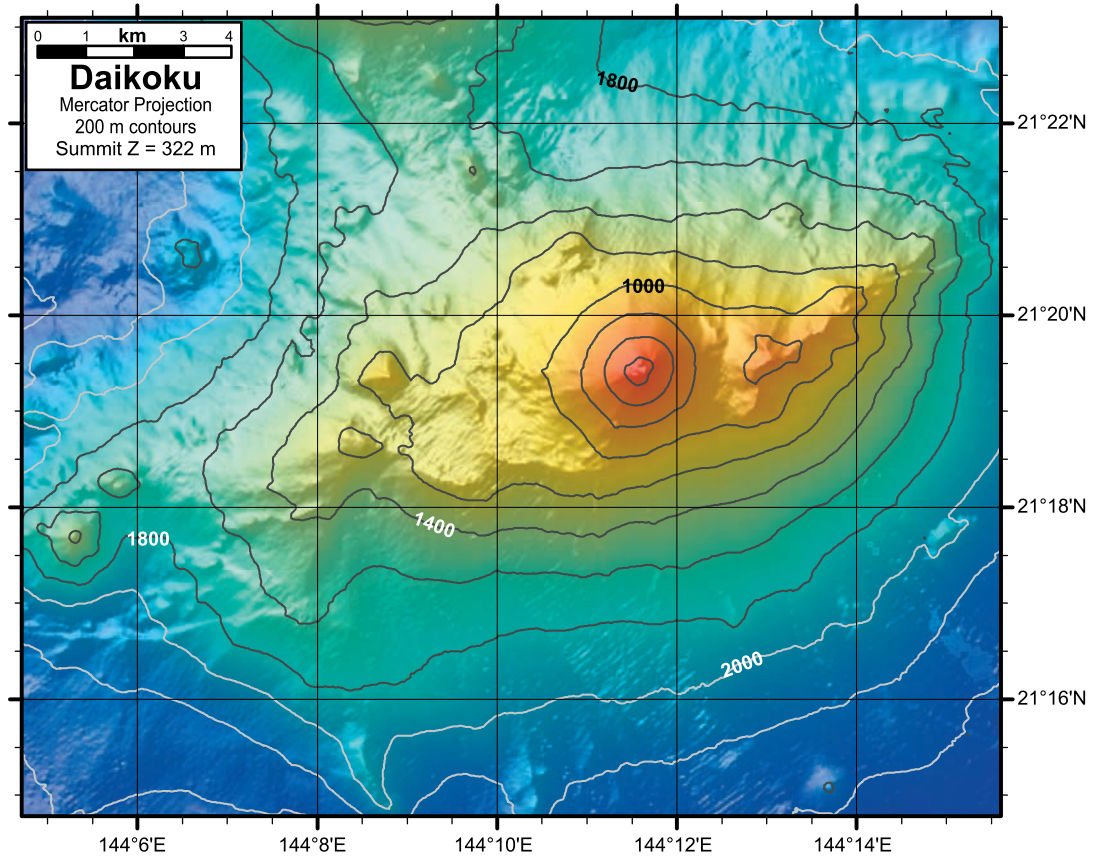**Figure 3.** Bathymetric maps showing locations of submarine arc volcanoes, including a detailed map showing vent locations. (a) NW Rota-1, (b) Daikoku, (c) NW Eifuku, (d) Nikko, (e) Giggenbach, and (f) Volcano-1. The high-resolution bathymetry in the detailed map of NW Eifuku was collected using the Imagenex sonar system mounted on the ROPOS ROV [*Chadwick et al.*, 2001, 2004].
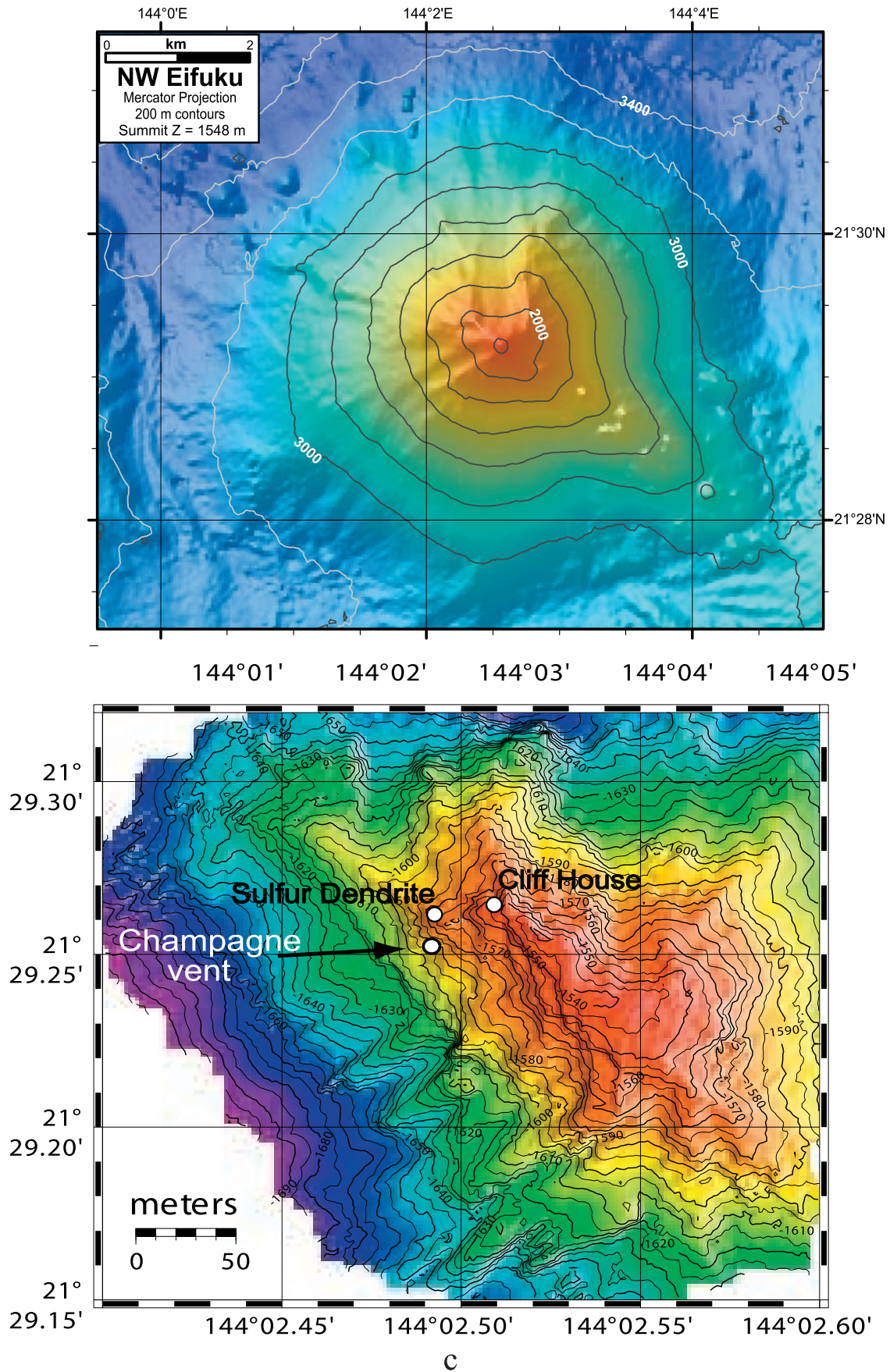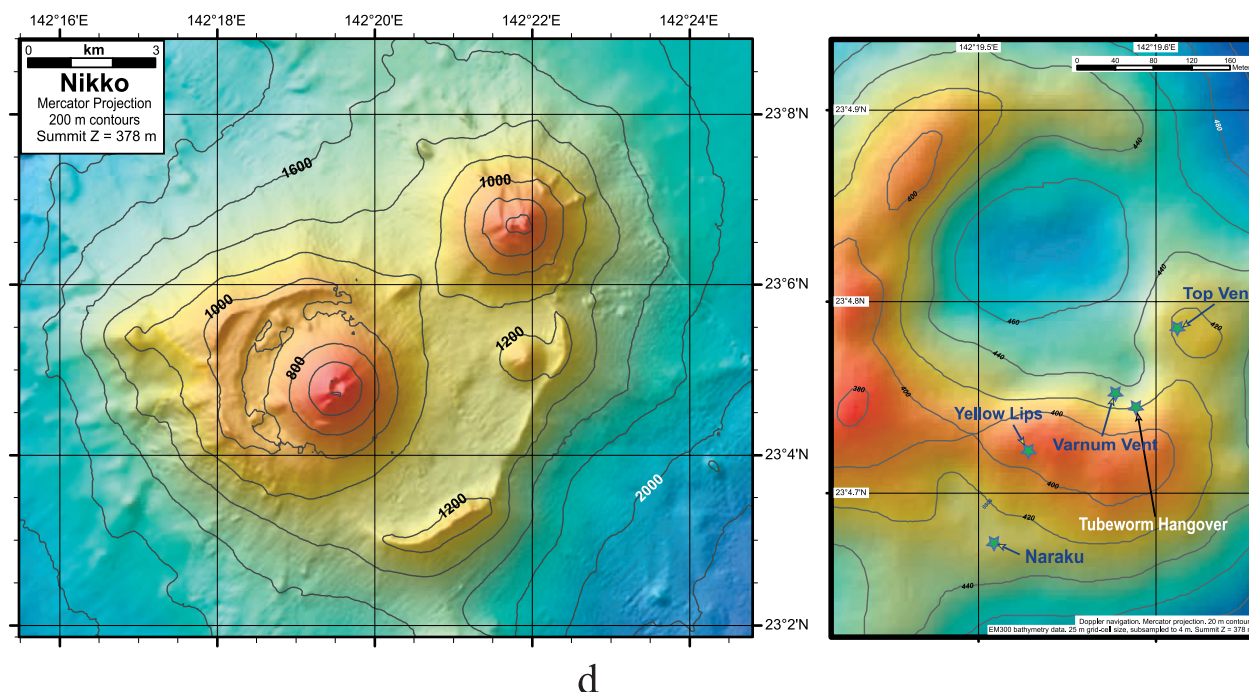
Figure 3. (continued)

Figure 3. (continued)

d

Figure 3. (continued)

seawater quenching, and was sloshing vigorously as it degassed [*Embley*, 2006; *Embley et al.*, 2007]. Our Daikoku samples came from a pit (Bubble Bath) containing fluid at 52°C that was also vigorously venting gas bubbles (Figure 4c). Jason 2 was able to collect several good fluid samples from Bubble Bath as well as one excellent gas sample using the inverted funnel in combination with our small volume gas-tight bottle. As shown in Table 1, the Bubble Bath gas was composed of ~94% CO$_2$ with only trace amounts of CH$_4$ and H$_2$. We did not analyze for sulfur gases, but considering the prevalence of sulfur deposits and liquid sulfur pools in the area, it is likely that the remaining 6% of the gas at Bubble Bath is a combination of H$_2$S and SO$_2$.
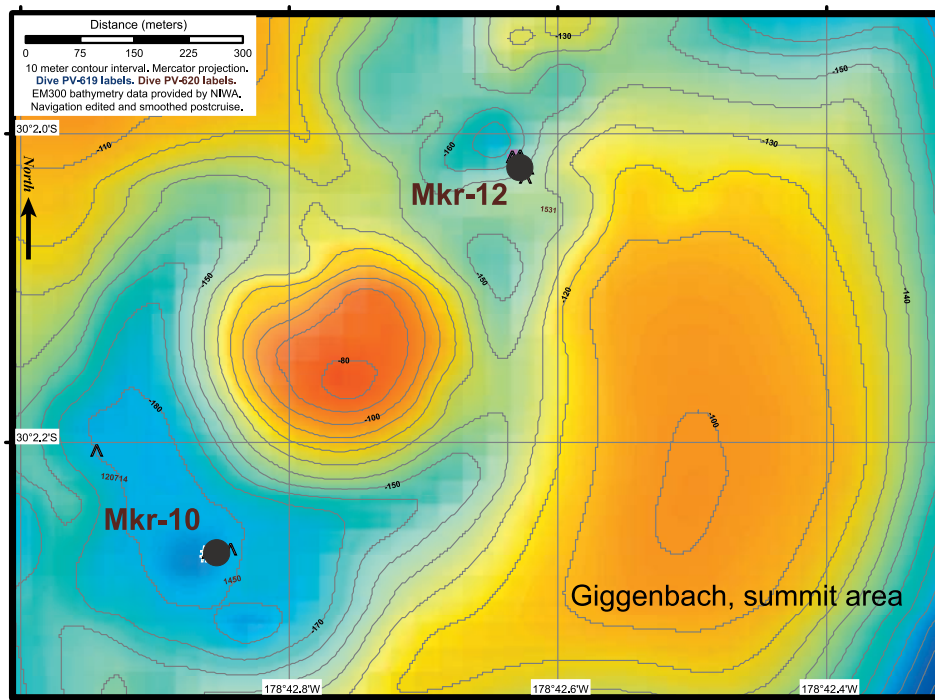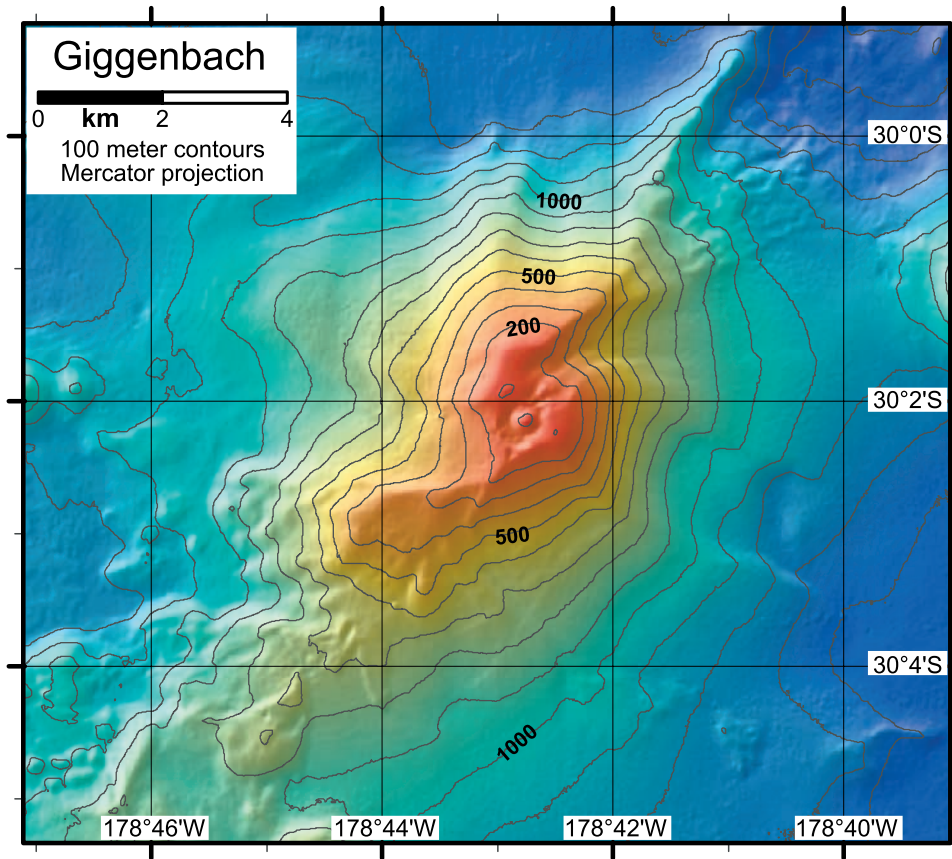
4.3. NW Eifuku

[15] NW Eifuku, a small volcanic cone located at 21.49°N, 144.04°E on the northern Mariana Arc, rises to a depth of ~1555 m below sea level (Figure 3c). ROPOS dives in 2004 discovered the impressive Champagne vent site at 1604 m depth venting streams of liquid CO$_2$ droplets as well as ~100°C hydrothermal fluid (Figure 4d). The venting on NW Eifuku has been described in some detail [*Lupton et al.*, 2006], but it is included here because it is perhaps the best example of a submarine arc volcano venting a separate CO$_2$ phase. The CO$_2$ at NW Eifuku takes the form of liquid droplets rather than gas bubbles due to the greater depth of the Champagne site. (Under oceanic conditions, CO$_2$ liquifies at a pressure of about 50 bars or ~500 m depth). Among other things, because the areal extent of the Champagne site is so small, it was possible to estimate the carbon flux at 23 mol CO$_2$/s by carefully examining the ROV video [*Lupton et al.*, 2006]. This approximately equals the CO$_2$ flux from all of the Endeavor Ridge vent fields on the Juan de Fuca Ridge, or about 0.1% of the global MOR carbon flux. In contrast, the CO$_2$ flux

from the 100°C Champagne vent fluids is estimated at ~0.5 mol/s, only 2% of the total flux. It was also found that the flux of liquid droplets increased dramatically whenever the seafloor around the Champagne site was disturbed by the ROV. This is consistent with the presence of a layer of liquid CO$_2$ beneath the surface capped by an impeding layer of CO$_2$ hydrate. These observations are similar to those reported at the Okinawa Trough back-arc basin, another site of liquid CO$_2$ venting [*Sakai et al.*, 1990a, 1990b].

[16] ROV dives were completed on NW Eifuku in 2004, 2005, and 2006, although the 2006 results are not included here. We were able to collect samples of the liquid CO$_2$ in 2004, but our seagoing vacuum line was overwhelmed by the quantity of gas contained in a gas-tight bottle filled with liquid CO$_2$. For this reason our best samples were collected in 2005. In preparation for the 2005 dives on NW Eifuku, we constructed two special small volume (~10 cm^3) versions of our gas-tight bottles for sampling the CO$_2$ liquid. By using these small volume bottles in conjunction with a special droplet catcher (Figure 2a), we were able to collect several excellent samples of the Champagne droplets. As shown in Table 1, the droplets are essentially pure CO$_2$ (98–100%). The Champagne vent fluid is also impressive, with many samples from both 2004 and 2005 containing ~600 mmol CO$_2$/kg, and two samples from 2004 containing 2.3–2.7 mol CO$_2$/kg. Since this is almost twice the CO$_2$ solubility of ~1 mol/kg in seawater at 100°C and 160 bars pressure, *Lupton et al.* [2006] attributed these high dissolved CO$_2$ values to the entrainment of small amounts of CO$_2$ hydrate or CO$_2$ liquid into the stream of rising vent fluid.
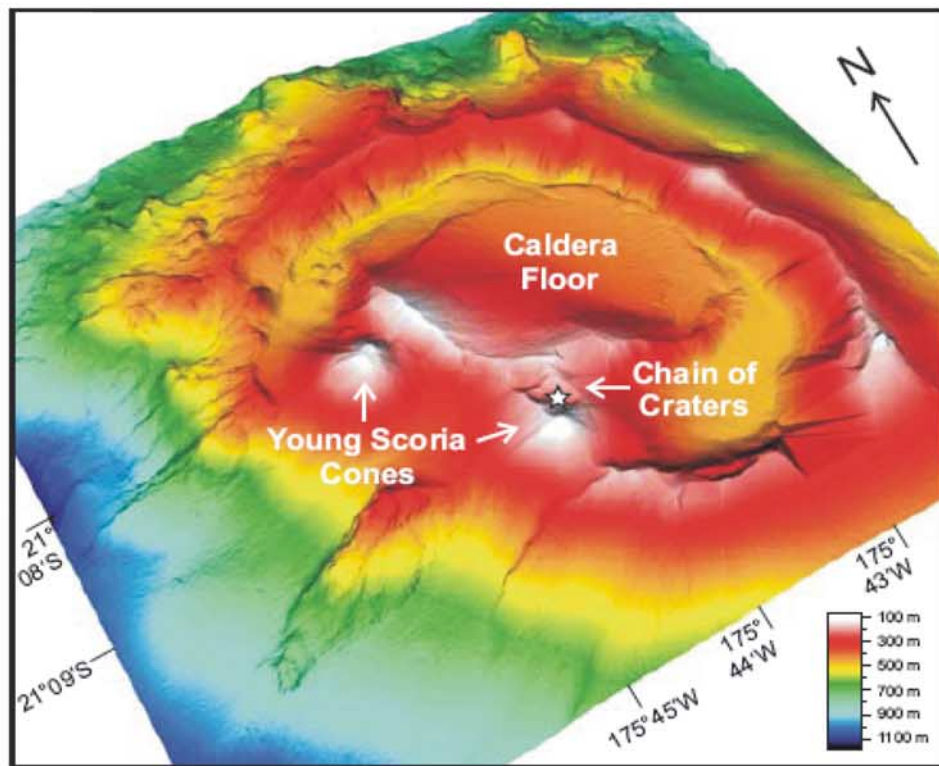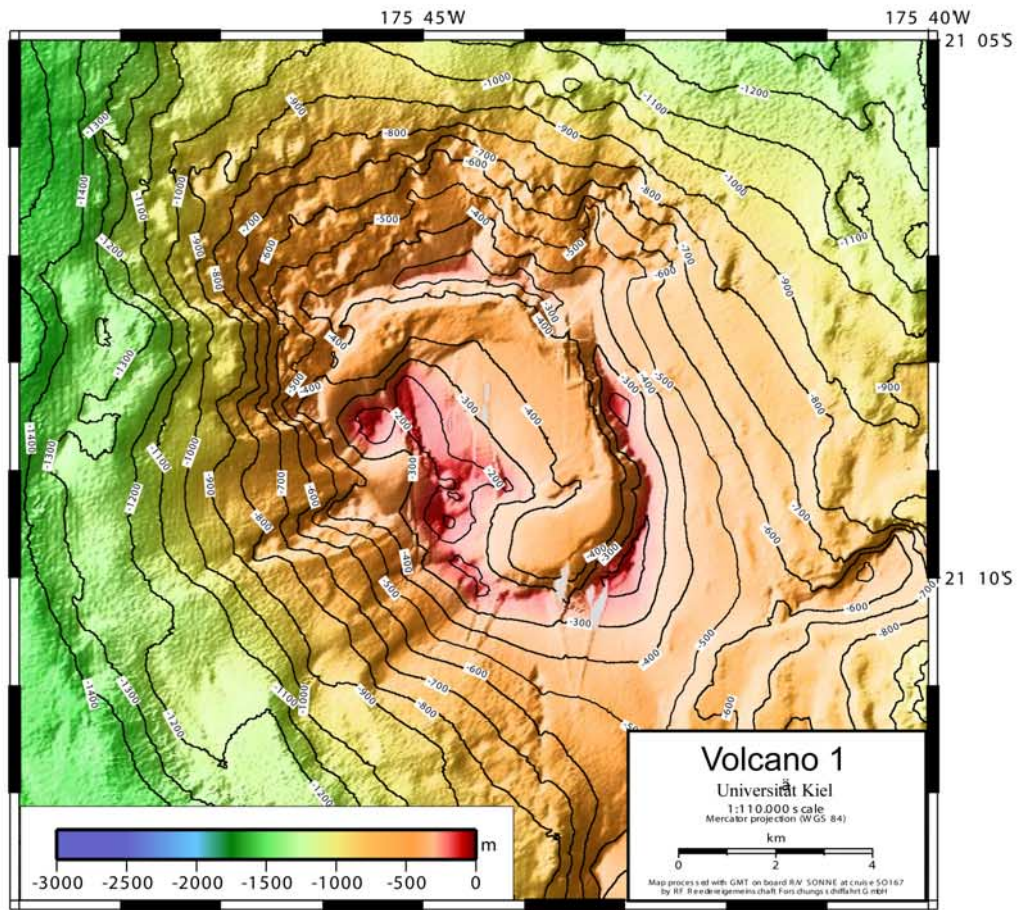
4.4. Nikko

[17] Nikko, located at 23.08°N, 142.33°E, is the north-ernmost of the Mariana Arc volcanoes studied during the
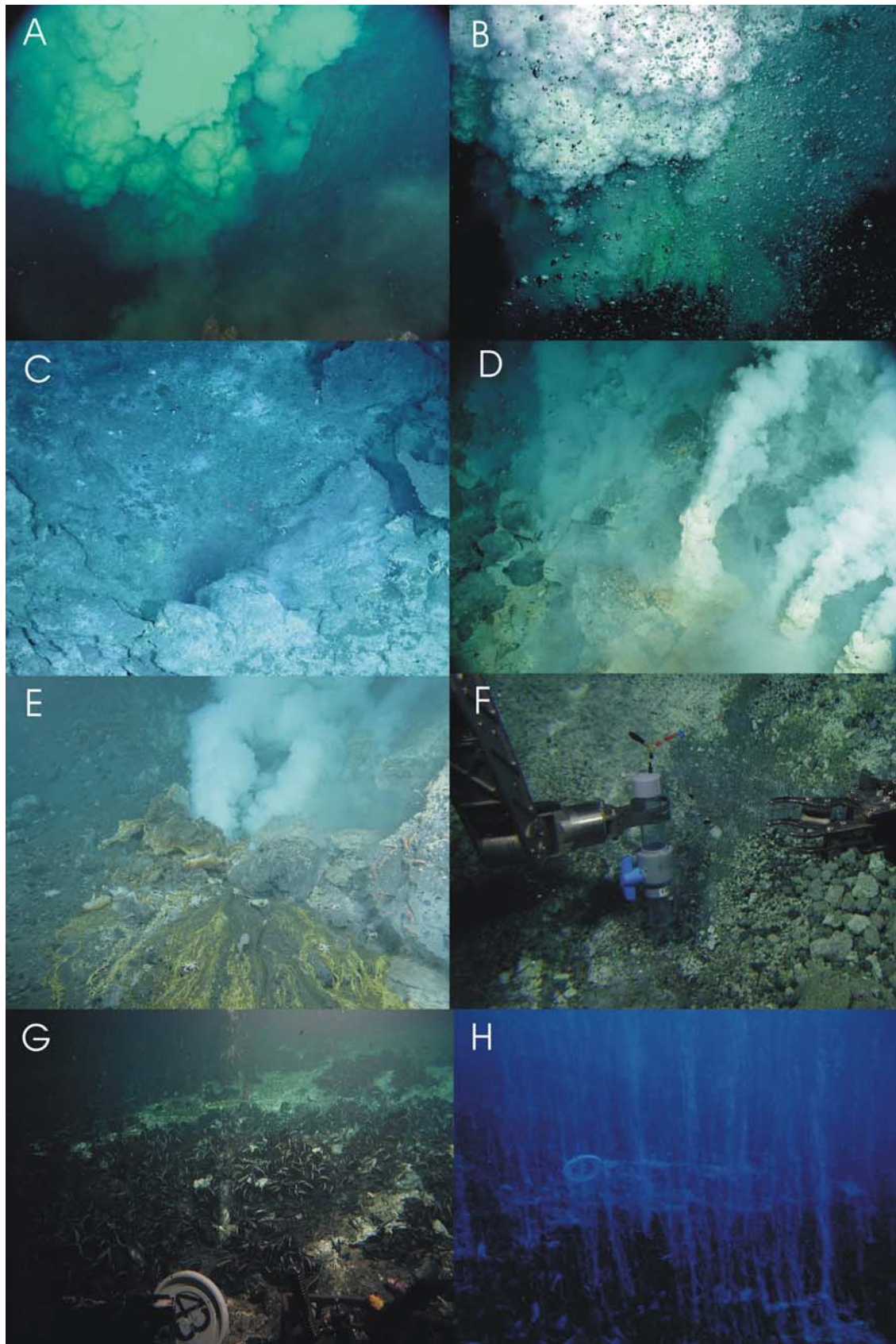
Figure 3. (continued)

Figure 3. (continued)

Figure 4

SRoF project. Nikko rises to a depth of about 365 m below sea level with a well-defined caldera at its summit (Figure 3d). The caldera floor is about 470 m below sea level. Three Hyper-Dolphin dives were completed on Nikko in 2005, followed by two Jason 2 dives in 2006. The very first dives on Nikko found the caldera densely populated with crabs and filled with white clouds of hydrothermal effluent. Several sites of hydrothermal venting were present, but perhaps most impressive were the pools of molten sulfur discovered by the Hyper-Dolphin [*Nakamura*, 2005]. At one site, hydrothermal fluid venting was present combined with CO_2 gas bubbling up through a pond of molten sulfur (Figure 4e). Hydrothermal fluid samples were collected at a variety of vents ranging from 60 to 215°C. One gas sample was collected in 2005 using the gas-tight bottle/inverted funnel technique (Figure 2c), yielding a composition of 96% CO_2 (Table 1). The low N_2 concentration in this sample indicates very little air contamination, and suggests that this method is perhaps the best approach for collecting high-quality samples of a separate gas phase.

4.5. Giggenbach

[18] Giggenbach volcano, named for the late New Zealand geochemist Werner Giggenbach, is located at 30.04°S, 178.71°E on the Tonga-Kermadec Arc. The volcano rises to a summit depth of about 80 m below sea level (Figure 3e). The three *Pisces V* dives devoted to exploring Giggenbach in 2005 found hydrothermal venting at two distinct sites at depths of about 160–190 m in pits on opposite sides of the summit cone [*Merle et al.*, 2005]. The Marker 10 site SW of the summit was venting fluid at 99–164°C that included a separate gas phase. Our best samples came from the Marker 12 site NW of the summit cone which was venting a mixture of fluid and gas bubbles at 204°C, right at the boiling point for this depth (176 m) (Figure 4f). We concluded that the fluid was boiling right at the Marker 12 vent orifice, promoting the formation of a separate gas phase. We collected two good samples of the gas bubbles at Marker 12 on successive dives (Table 1). While it was possible to obtain uncontaminated samples of the gas phase using the plastic cylinder, sampling the fluid was much more difficult, due to contamination with gas bubbles located in the fluid stream. After correction for air addition on the basis of the N_2 and Ar concentrations, the gas bubbles at Giggenbach were composed of 94–98% CO_2 with only trace amounts of H_2 and CH_4 (Table 1).

4.6. Volcano-1

[19] Volcano-1, located at 21.15°S 175.75°E, was one of three volcanoes on the Tonga-Kermadec Arc sampled during the German SITKAP expedition in June 2005 [*Stoffers et al.*, 2005, 2006]. Additional samples were collected in May 2007 with the ROV ROPOS from the

R/V *Sonne*. As reported by *Stoffers et al.* [2006], Volcano-1 rises to within 65 m of the sea surface, and has a large caldera and several small cones at its summit (Figure 3f). During the five dives devoted to exploring the volcano, *Pisces IV* discovered widespread areas of diffuse venting (50–150°C) within the caldera at depths of 160–210 m. Continuous streams of gas bubbles were observed in several areas (Figures 4g and 4h), and large areas of the caldera floor were covered with fields of mussels. We obtained several vent fluid samples with the gas-tight bottles at temperatures ranging from 50 to 150°C, and two excellent samples of gas bubbles collected with the plastic cylinder scoop. The composition of the gas phase was essentially 100% CO_2 (Table 1).

5. Helium-Carbon Relationships

[20] Some insight into the origin of the gases and gas-rich fluids emanating from submarine volcanoes can be gained by focusing on the magmatic gases CO_2 and ^3He. ^3He is completely inert and derived from magma, while CO_2 is very unreactive and derived almost entirely from a magmatic source. These two species are distinct from other gases such as H_2, CH_4, H_2S, and SO_2 which may be partly derived from magmatic gas, but are also highly reactive and therefore not diagnostic of gas sources.

[21] The histograms in Figure 5 compare the CO_2 concentrations for the six arc volcanoes discussed here with CO_2 in typical MOR systems. In addition, Figure 5 (bottom) shows total gas concentrations for those volcanoes from the Mariana and Tonga-Kermadec arcs that are not venting a separate gas phase. It should be noted that the values plotted for MOR systems are estimated end-member concentrations based on extrapolation to zero Mg, while those for the arc volcanoes have not been corrected and are thus lower limits. Furthermore, the MOR systems that are shown in the histogram are either from fast spreading ridges or ridges that have been affected by recent magmatic input and thus have higher than average CO_2 concentrations. Although there is a large variation in the concentration values both among the various volcanoes and within each volcano, this comparison makes it clear that the CO_2 concentrations at these submarine arc volcanoes are much higher than those found on mid-ocean ridges. For example, the maximum vent fluid CO_2 concentrations at NW Rota-1, Daikoku, NW Eifuku, Nikko, Giggenbach, and Volcano-1 are 93, 38, 2700, 68, 366, and 133 mmol/kg, respectively (Table 1). These concentrations are much higher than the typical values found at MOR hydrothermal systems, which range between 3 and 200 mmol/kg, with most of the MOR vent fluid samples having $[CO_2]$ less than 30 mmol/kg (Figure 5). Furthermore, comparison with Figure 5 (bottom) shows that the arc volcanoes venting a separate CO_2-rich gas phase

Figure 4. Photographs of submarine arc volcanoes. (a) Eruptive activity at Brimstone Pit, NW Rota-1 in 2004. (b) Brimstone Pit, NW Rota-1 in 2006, showing gas bubbles and red erupting lava. (c) Bubble Bath vent on Daikoku, 2006. (d) Champagne Vent, NW Eifuku, showing 100°C fluid venting from small white chimneys and cold liquid CO_2 droplets rising from the seafloor. (e) A sulfur pool vent on Nikko showing sulfur flows, hot fluid venting, and CO_2-rich gas bubbles. (f) The *Pisces* submersible collecting a gas sample at Giggenbach Marker 12 using the plastic cylinder. At this vent the gas bubbles and vent fluid were commingled in a single stream. (g) Stream of gas bubbles rising from a bed of mussels at Volcano-1. (h) Multiple streams of CO_2-rich gas bubbles rising from the seafloor on Volcano-1.

Table 1. Gas Compositions for Vent Fluids and Gas Phase Samples From NW Rota-1, Daikoku, NW Eifuku, Nikko, Giggenbach, and Volcano-1[a]

Sample	Vent	Collection	Temp (°C)	Mg	CO$_2$	CH$_4$	H$_2$	N$_2$	Ar	He (μmol kg^{-1})	Ne (μmol kg^{-1})	He[b] (μmol kg^{-1})	^{3}He/^{4}He[b] (R/R$_A$)	C/^{3}He[b]	C/^{3}He[b] Corr[c]
NW Rota-1															
R783-GT9	Fault Shrimp	3/29/04	21.5	53.44	37.6	0.0034	0.0001	1.34	0.0265	0.516	0.032	0.507	8.35	6.4E+09	6.0E+09
R783-GT11	Scarp Top	3/29/04	39	49.43	93.5	0.0099	0.0578	1.07	0.0186	1.19	0.021	1.18	8.31	6.8E+09	6.7E+09
R783-GT7	Iceberg	3/29/04	45	51.3	77.7	0.0024	0.0002	0.892	0.0164	1.12	0.017	1.12	8.32	6.0E+09	5.8E+09
R783-GT2	High Flow	3/29/04	36.5	52.18	18.0	0.00064	0.0033	4.75	0.0248	0.32	0.106	0.29	8.12	5.5E+09	4.8E+09
R786-GT11	Brimstone pit	4/2/04	27.5	51.47	25.0	0.00022	0.154	0.411	0.0102	0.174	0.006	0.172	8.23	1.3E+10	1.2E+10
R786-GT9	Brimstone pit	4/2/04	26	51.52	21.5	0.00023	0.293	0.719	0.0104	0.300	0.015	0.296	8.23	6.4E+09	5.7E+09
R786-GT5	Shim Sands	4/2/04	62	41.57						0.459	0.055	0.443	8.1		
J2-187-GT15	Brimstone Pit	4/23/06	25	51.29	7.63	0.00002	0.0651	0.612	0.0200	0.0368	0.010	0.0339	8.30	2.0E+10	1.4E+10
J2-187-GT5	Brimstone Pit	4/23/06	95	47.72	18.3	0.00003	1.291	0.647	0.0219	0.178	0.011	0.175	8.27	9.1E+09	8.0E+09
J2-187-GT6	Iceberg	4/23/06	50	51.52	21.9	0.00078	0.00014	0.611	0.0231	0.266	0.097	0.263	8.29	7.2E+09	6.5E+09
J2-188-GT5	Brimstone Pit 1 cm in sand	4/24/06	120	48.72	52.2	0.00003	2.187	0.708	0.0225	0.669	0.0126	0.666	8.27	6.8E+09	6.5E+09
J2-188-GT15	Brimstone Pit fluid S smoke	4/24/06	95	47.62	80.3	0.00006	1.274	0.514	0.0170	0.372	0.082	0.370	8.23	1.9E+10	1.8E+10
J2-189-GT6	Brimstone Pit fluid without bubbles in S8 smoke, edge of flow	4/25/06	120	51.22	47.0	0.00007	1.192	0.314	0.0124	0.427	0.050	0.425	8.27	9.6E+09	9.2E+09
J2-188-GT2	Brimstone[d]	4/24/06			92.5	0.00004	10.7	0.221	0.00518	32.38	0.0255	32.38	8.27	2.5E+09	—
J2-189-GT11	Brimstone Pit gas[d]	4/25/06			89.2	0.00017	12.6	0.243	0.00636	38.11	0.0280	38.11	8.28	2.0E+09	—
Daikoku															
Hyp 491-GT7	Bottomless pit	10/26/05	16	51.13	2.45	0.00004	0.000185	10.6	0.0427	0.0430	0.205	—	—	—	
Hyp 491-GT6	Bottomless pit	10/26/05	16	50.82	2.04	0.00003	0.000258	4.96	0.0539	0.0183	0.0926	—	—	—	
J2-195-GT15	Bubble Bath	05/02/06	52	46.39	38.0	0.00025	0.000686	0.478	0.0155	0.0395	0.0804	0.0372	7.37	9.9E+10	9.3E+10
J2-195-GT2	White smoker 2nd orifice	05/02/06	210	48.67	14.17	0.00025	0.000396	0.543	0.0188	0.0355	0.0089	0.0329	7.42	4.2E+10	3.5E+10
J2-197-GT2	Bubble field also near S8 Pit	05/04/06	55	48.52	22.0	0.00023	0.0116	33.5	0.140	0.264	0.710	0.0591	—	3.6E+10	3.3E+10
J2-197-10cc 1	Bubble Bath gas[d]	05/04/06	—	—	94.02	0.00511	0.00181	0.552	0.0147	9.62	0.081	9.62	7.41	9.5E+09	—
NW Eifuku															
R791-GT7	Champagne	4/9/04	103	52.52	118	0.0138	0.00011	1.01	0.0194	0.475	0.0182	0.472	7.33	2.5E+10	2.3E+10
R791-GT9	Champagne[e]	4/9/04	103	45.11	2308										
R791-GT11	Champagne[e]	4/9/04	103	43.93	2711										
R793-GT5	Champagne	4/11/04	68	46.85	254	0.00017	0.00071	1.63	0.0168	0.386	0.0325	0.379	7.33	6.6E+10	6.0E+10
R793-GT11	Sulfur Dendrite	4/11/04	48	50.43	306	0.0137	0.00019	0.48	0.0075	0.843	0.0077	0.843	7.22	3.6E+10	3.6E+10
R793-GT7	Cliff House	4/11/04	49	49.20	703								7.32		
R791-GT2	Diffuse Site	4/9/04	11	51.19	76.0	0.0111	0.00010	1.56	0.0265	0.460	0.0301	0.454	7.34	1.6E+10	1.6E+10
H494-GT4	Champagne	10/29/05	68	47.14	564	0.00127	0.108	7.35	0.0583	0.652	0.132	0.614	7.26	9.1E+10	9.3E+10
H497-GT10	Champagne, 2nd Site	11/1/05	56–63	49.12	136	0.00021	0.00326	0.69	0.0599	0.172	0.012	0.168	7.29	8.0E+10	7.9E+10
H497-GT16	Champagne, 2nd Site	11/1/05	63	51.48	72.3	0.00016	0.00089	0.96	0.0141	0.077	0.014	0.073	7.31	9.7E+10	9.4E+10
H497-GT6	Champagne	11/1/05	108	46.22	405	0.00059	0.00588	1.03	0.0120	0.621	0.027	0.613	7.25	6.6E+10	6.5E+10
H497-GT7	Champagne	11/1/05	103	43.53	591	0.00169	0.0123	36.0	1.21	1.07	0.879	0.819	7.22	7.2E+10	7.2E+10

Table 1. (continued)

Sample	Vent	Collection	Temp (°C)	Mg	CO_2	CH_4	H_2	N_2	Ar	He (µmol kg⁻¹)	Ne (µmol kg⁻¹)	He[b] (µmol kg⁻¹)	$^3He/^4He$[b] (R/R$_A$)	$C/^3He$[b]	$C/^3He$[b] Corr[c]
H499-GT5	Champagne	11/2/05	47	48.64	174	0.00041	0.00181	1.01	0.0126	0.259	0.017	0.254	7.28	6.8E+10	6.6E+10
H499-GT15	Cliff House	11/2/05	64	44.94	567	0.0136	0.00316	1.15	0.0133	2.08	0.029	2.07	7.26	2.7E+10	2.7E+10
H492-10cc#1	Champagne droplets[d]	10/27/05	<4		98.7	0.00064	0.00032	0.081	0.00034	5.15	0.0123	5.15	7.31	1.9E+10	—
H494-10cc#1	Champagne droplets[d]	10/29/05	<4		98.6	0.00092	0.00017	0.206	0.00103	5.72	0.0460	5.72	7.33	1.7E+10	—
H497-10cc#2	Champagne droplets[d]	11/1/05	<4		99.6	0.00088	0.00023	0.224	0.00114	5.37	0.0474	5.37	7.30	1.8E+10	—
H499-10cc#1	Champagne droplets[d]	11/2/05	<4		98.9	0.00094	0.00023	0.140	0.00128	6.99	0.0161	6.99	7.30	1.4E+10	—
Nikko															
Hyp 496-GT15	Nikko, stn 2	10/31/05	112	38.04	58.7	0.0019	0.0011	1.13	0.0204	0.296	0.0188	0.290	6.77	2.2E+10	2.1E+10
Hyp 496-GT5	Nikko, stn 3	10/31/05	107	50.65	3.53	0.00013	0.0006	0.631	0.0121	0.0083	0.0094	0.0056	—	6.7E+10	2.5E+10
Hyp 496-GT9	Nikko, stn 3	10/31/05	107	51.19						0.0040	0.0081	0.0017	—		
Hyp 500-GT7	Nikko deployment site	11/3/05	108	40.28	71.7	0.0017	0.0024	1.32	0.0153	0.360	0.0173	0.355	6.77	2.0E+10	1.9E+10
Hyp 500-GT6	Nikko deployment site	11/3/05	108	40.68	140	0.00036	0.0047	13.2	0.0323	0.391	0.0205	0.386	6.81		
Hyp 500-GT16	Nikko southern lone vent	11/3/05	90	47.27	26.4	0.00021	0.0396	26.3	0.407	0.233	0.2729	0.154	—		
Hyp 500-GT10	Nikko	11/3/05	61–68	46.76	67.7	0.00174	0.0045	15.4	0.356	0.224	0.625	0.044	—	6.4E+10	5.8E+10
Hyp 501-GT15	Nikko deployment site	11/4/05	110	39.87						0.439	0.3577	0.336	6.79	2.1E+10	2.1E+10
J2-198-GT11	N Nikko	5/7/06	215	46.19	25.3	0.00013	0.00056	0.608	0.0182	0.0447	0.0112	0.0415	6.88	6.4E+10	5.8E+10
Hyp 500-GT17	Nikko gas bubble[d]	11/03/05	—	—	96.50	0.0033	0.00077	1.057	0.0181	18.5	0.11	18.5	6.89	5.5E+09	—
Giggenbach															
P5-618-GT2	Diffuse SW flank	04/15/05	72.3	47.39	3.815	0.00120	0.00006	0.512	0.0175	0.057	27.3	0.049	7.37	7.6E+09	3.1E+09
P5-618-GT11	Summit mussel bed	04/15/05	70.4	52.35	361	0.0161	0.0856	3.43	0.0799	0.050	9.0	0.048	7.48	2.3E+09	2.3E+09
P5-619-GT12	Giggenbach mk12	04/16/05	203	34.15						15.0	54.5	15.0	7.42		
P5-619-GT6	Giggenbach mk12	04/16/05	203	28.18						14.3	59.8	14.3	7.43		
P5-619-GT7	Giggenbach mk12	04/16/05	203	30.70	177	0.015	0.063	1.066	0.045	8.78	66.5	8.76	7.44	2.0E+09	
P5-620-GT11	Giggenbach mk10	04/17/05	165	51.18	4.42	0.00057	0.00136	0.656	0.0149	0.057	13.1	0.053	7.49	8.0E+09	
P5-620-GT2	Giggenbach mk12	04/17/05	203	52.6	2.23	0.00047	0.00091	0.093	0.0013						
P5-620-GT12	Giggenbach gas[d]	04/17/05			77.5	0.0134	0.0330	4.81	0.0721	53.8	1.56	53.4	7.41	1.3E+09	—
P5-620-GT6	Giggenbach gas[d]	04/17/05			88.9	0.0063	0.0226	5.45	0.0725	57.0	1.38	56.6	7.43	1.5E+09	—
P5-620-GT6	Giggenbach gas[d]	04/17/05			84.8	0.00743	0.0247	12.9	0.129	57.0	1.38	56.6	7.43		
P5-619-Fl. 22	Giggenbach mk12[d]	04/16/05								68.0	3.60	67.0	7.46		
P5-619-Fl. 17	Giggenbach mk12[d]	04/16/05													
Volcano-1															
P4-141-GT12	Vent Field	6/24/05	50	50.64	108	0.0306	0.014	5.54		0.397	0.0079	0.395	6.59	3.0E+10	2.9E+10
P4-141-GT10	Mussel Field	6/24/05	68	51.86	133	0.0216		0.649		0.481	0.0089	0.479	6.61	3.0E+10	3.0E+10
P4-142-GT6	Bubble Site	6/25/05	71	52.15	3.66	0.0005		1.63	0.0149	0.0087	0.0079	0.0064	6.95	5.9E+10	2.5E+10
P4-142-GT2	Mussel Bowl	6/25/05	150	51.46	4.68	0.00002	0.00003	0.451	0.0149	0.0732	0.0019	0.0727	6.88	6.7E+09	3.6E+09
R1050-GT10	Marker 43	5/11/07	64	52.1	177.0	0.0267	0.00060	1.167	0.0205	0.897	0.016	0.892	6.60	2.2E+10	2.1E+10
R1050-GT5	Bubbles Vent	5/11/07	39	54.8	37.0	0.0003	0.00042	0.492	0.0164	0.029	0.0098	0.026	6.71	1.5E+11	1.5E+11
R1051-GT15	Bubbles Vent	5/12/07	17	56.0	12.24	0.0004	0.00051	0.620	0.0170	0.106	0.0121	0.103	6.66	1.3E+10	1.1E+10
R1053-GT10	Sulfur Vent	5/14/07	36	55.2	42.44	0.0286	0.00014	0.774	0.0185	0.246	0.0143	0.242	6.68	1.9E+10	1.8E+10
P4-141-Fl.22	Mussel Field (gas)[d]	6/24/05	68							12.7	0.275	12.8	6.59		
P4-141-Fl.16	Mussel Field (gas)[d]	6/24/05	68		102	0.052	0.0253	1.27	0.0151	12.4	0.179	12.5	6.60	8.9E+09	—

Table 1. (continued)

Sample	Vent	Collection	Temp (°C)	Mg	CO_2	CH_4	H_2	N_2	Ar	He (μmol kg^{-1})	Ne (μmol kg^{-1})	He[b] (μmol kg^{-1})	^{3}He/^{4}He[b] (R/R$_A$)	C/^{3}He[b]	C/^{3}He[b] Corr[c]
P4-142-Fl.22	Mussel Bowl (gas)[d]	6/25/05	150		100	0.046	0.0253	1.90	0.0177	11.1	0.406	11.3	6.60	9.7E+09	–
P4-142-Fl.17	Mussel Bowl (gas)[d]	6/25/05	150							11.3	0.447	11.5	6.61		
R1051-GT7	Bubbles Vent (gas)[d]	5/12/07	17	–	98.33	0.0051	0.00087	1.39	0.0213	19.5	0.119	19.5	6.60	5.5E+09	
R1053-GT5	Marker 43 (gas)[d]	5/14/07	>60	–	97.70	0.0243	0.00056	0.725	0.0088	10.3	0.058	10.3	6.62	1.0E+10	

[a] Units are mmol/kg unless noted otherwise. For the conventional gas chromatograph analyses (CO_2, CH_4, H_2, N_2, Ar), the concentrations are precise to about ±5%. The vent fluid and gas samples have designations indicating the platform used for the collection: R (ROPOS), H (Hyper-Dolphin), J2 (Jason-2), P4 and P5 (Pisces-IV and Pisces-V), followed by the dive number.
[b] The ^{3}He and ^{4}He concentrations and ^{3}He/^{4}He ratios have had the effect of air addition subtracted out based on the Ne concentration and assuming that the added component had He/Ne = (He/Ne)air = 0.288.
[c] The C/^{3}He Corr has had the ^{3}He corrected for air addition and also the C corrected by subtracting out the seawater background of 2.2 mmol CO_2/kg.
[d] For the liquid droplet and gas bubble samples, we report the gas compositions as a volume % or ppm.
[e] Samples for which the gas content was more than our extraction system could easily handle, and some fractionation of the gases occurred. For this reason we are reporting only those gas compositions that are reliable.
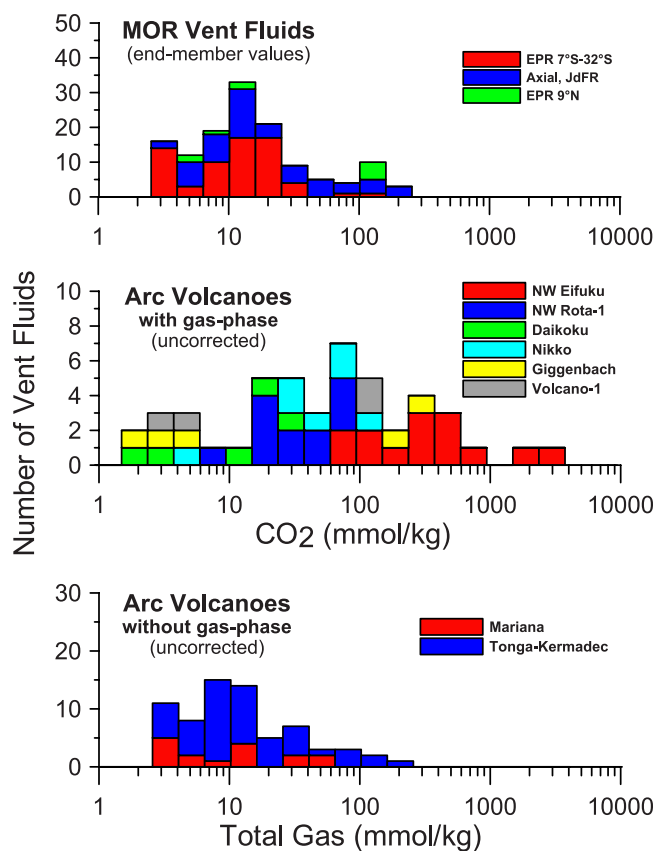

Figure 5. (top) Histogram comparing CO_2 concentrations in mid-ocean ridge (MOR) vent fluids [*Kelley et al.*, 2004], (middle) concentrations in the six arc volcanoes that have a separate gas phase, and (bottom) total gas concentrations in 16 other Mariana and Tonga-Kermadec volcanoes without a separate gas phase. The MOR vent fluid values are estimates of end-member concentrations based on extrapolating to zero Mg. The arc volcano values have not been corrected in any way and are thus lower limits. Because we do not have gas composition analyses for all the volcanoes studied, we have plotted total gas concentration in Figure 5 (bottom) as a proxy for CO_2 concentration, on the assumption that CO_2 is the most abundant gas.

have higher dissolved gas concentrations on the average compared to arc volcanoes without a free gas phase.

[22] Figure 6 shows plots of [^{3}He] versus [CO_2] for each of the six volcanoes that are the focus of this paper. In each plot the discrete data points indicate concentration data from the individual vent fluid samples, while the dashed lines indicate the C/^{3}He ratio for the separate gas phase sampled at each of these sites. Figure 6 shows that the relationship between CO_2 and ^{3}He in the dissolved fluid component is much different from that in the accompanying gas phase. For each volcano the gas component (dashed line) has a steeper slope than the fluid samples, indicating a lower C/^{3}He ratio in the gas phase compared to the fluid. In one sense this result is not surprising, since helium has a much lower solubility in water and seawater than CO_2. This effect is shown quite clearly in Figure 7, which plots the ratio $(CO_2/^3He)_{liquid}/(CO_2/^3He)_{gas}$ as a function of vent temperature. The lines indicate theoretical values for this ratio for
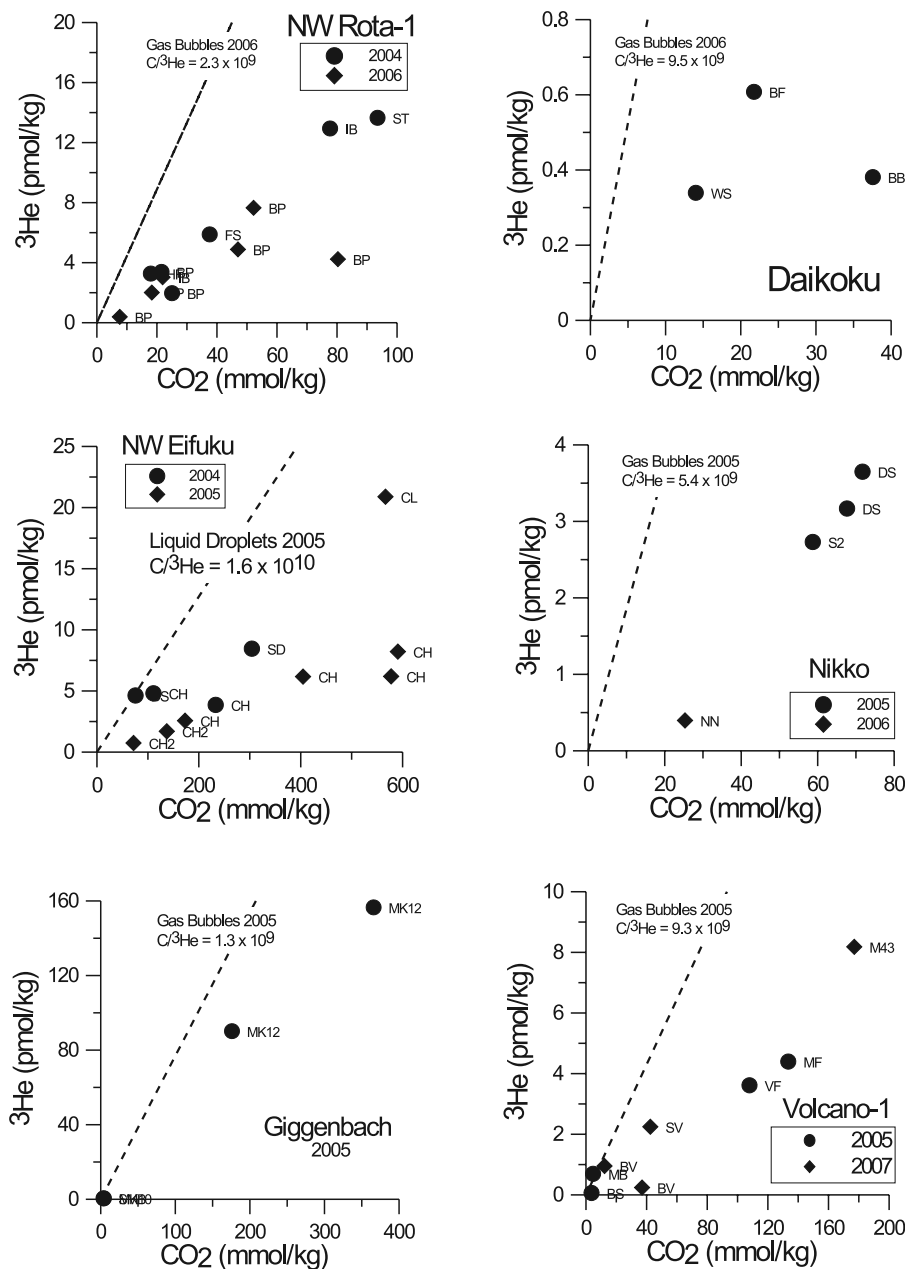
Figure 6. Plots of ^{3}He concentration versus CO$_2$ concentration for NW Rota-1, Daikoku, NW Eifuku, Nikko, Giggenbach, and Volcano-1. Filled symbols are vent fluid dissolved gas concentrations. Dashed line indicates the C/^{3}He slope for the associated gas phase. The abbreviations next to the symbols refer to the individual vents listed in Table 1.

pure water at various pressures spanning the depth range of interest from 100 to 1500 m (10 to 150 bars). The theoretical curves are equivalent to $\beta(CO_2)/\beta(He)$, where β is the Bunsen solubility coefficient. The theoretical curves thus indicate the values which should obtain if there were perfect equilibrium between the gas and liquid for both CO$_2$ and ^{3}He.

[23] Figure 7 shows that the ratio (CO$_2$/^{3}He)$_{liquid}$/ (CO$_2$/^{3}He)$_{gas}$ falls between 2 and 10 for most of the hydrothermal fluids on these six volcanoes. However, the theoretical values of (CO$_2$/^{3}He)$_{liquid}$/(CO$_2$/^{3}He)$_{gas}$ are considerably higher, starting at values of 30 to 160 at 0°C and decreasing slowly to ~5 at higher temperatures. While the

measured values show considerable scatter, there is no discernible trend versus temperature or depth. The discrepancy between the measured and theoretical values of (CO$_2$/^{3}He)$_{liquid}$/(CO$_2$/^{3}He)$_{gas}$ suggests either lack of equilibration between the gas and liquid phases, or that equilibration occurred at a much higher temperature than measured at the vent orifice. As we will discuss later, other results also indicate disequilibrium between the gas and liquid phases.

[24] Gases emanating from volcanic arcs typically have C/^{3}He ratios elevated relative to gases from mid-ocean ridge hydrothermal systems [*Sano and Williams*, 1996; *van Soest et al.*, 1998]. This is attributed to the assimilation of organic
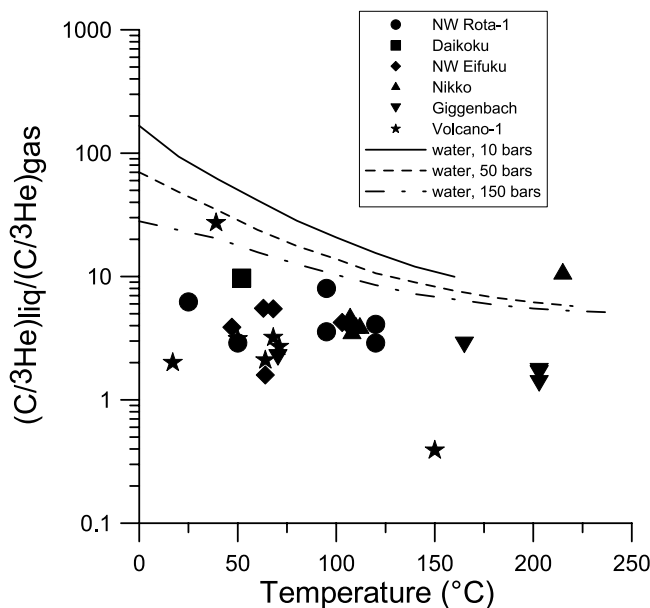
Figure 7. Plot of the ratio (CO$_2$/^{3}He)$_{liquid}$/(CO$_2$/^{3}He)$_{gas}$ versus temperature for vent fluids (filled symbols). For comparison, the solid and dashed lines show theoretical values for this ratio in pure water at various pressures spanning the depth range from 100 to 1500 m (10 to 150 bars). For this calculation we used the model of *Duan and Sun* [2003] and Z. H. Duan (report, 2006) for CO$_2$ and data from *Wiebe and Gaddy* [1935] and *Baranenko et al.* [1989] for helium. This ratio indicates the relative partitioning for CO$_2$ and He between the liquid and gas phases, and for the theoretical curves it is equivalent to β(CO$_2$)/β(He), where β is the Bunsen solubility coefficient. We have assumed that the solubility coefficient for ^{3}He is the same as that for He, since it has been shown that the solubility of the two isotopes differ only by a few percent at temperatures up to 20°C [*Weiss*, 1970; *Top et al.*, 1987]. We have used values for pure water since very few solubility data are available for He in NaCl solutions at elevated temperatures and pressures. However, the data of *Weiss* [1971, 1974] indicate almost no difference in β(CO$_2$)/β(He) for seawater versus pure water at temperatures between 0 and 40°C at 1 atm pressure. Another comparison using data from *Gardiner and Smith* [1972], *Gerth* [1983], and Z. H. Duan (report, 2006) shows no appreciable difference in β(CO$_2$)/β(He) in pure water versus 1.0 m NaCl solution at pressures up to 600 bars and temperatures up to 100°C.

matter and marine carbonates into the subducting slab and subsequently into the arc magmas. For volcanic arcs, C/^{3}He ratios typically fall in the range of 10^{10}–10^{13}, while MOR vent fluids have lower C/^{3}He values averaging 1–2×10^9 [*Resing et al.*, 2004; *Kelley et al.*, 2004]. The six arc volcanoes we are examining in this paper follow this general pattern. As summarized in Figure 8, the vent fluid C/^{3}He ratios in the present study range from 3×10^9 for Giggenbach up to 8×10^{10} for Daikoku and NW Eifuku, with most of the samples having C/^{3}He > 6×10^9.

[25] In addition to the C/^{3}He ratio, the C isotopic ratio of the CO$_2$ can also provide insights into the origin of the carbon. Mid-ocean ridge systems typically have δ^{13}C(CO$_2$)

in the range of −13 up to −4 ‰, while typical arcs have heavier δ^{13}C closer to the values found in marine carbonates (−2 to +1‰)[*Kelley et al.*, 2004; *Sano and Williams*, 1996; *van Soest et al.*, 1998; *Hoefs*, 1980]. As reported previously by *Lupton et al.* [2006], the NW Eifuku vent fluids had δ^{13}C (CO$_2$) averaging −1.75‰, while the liquid droplets were slightly heavier (−1.2 to −1.28‰). For the six volcanoes discussed here, the only other carbon isotope analysis that has been completed (measured at the Univ. of Otago, New Zealand) was at Giggenbach, where the CO$_2$ dissolved in the boiling 202°C vent fluid at the Marker 12 site had δ^{13}C of −1.3‰. Thus the carbon isotope signatures in the CO$_2$ at NW Eifuku and at Giggenbach are very similar even though these volcanoes are located on different volcanic arcs.

6. Solubility Considerations

[26] In each of the six volcanoes we have examined here, a free gas phase is present in combination with venting of conventional hydrothermal fluids. In each case the gas phase consists of essentially pure CO$_2$ (>90% by volume). If the CO$_2$ dissolved in these hydrothermal fluids is in solubility equilibrium with the CO$_2$ gas phase, then that would imply that the gas was exsolving from the fluid at a shallow depth near the vent orifice. A simple way to address this question is to directly compare the CO$_2$ concentrations measured in the vent fluids with the expected saturation concentration for pure CO$_2$ for the p,T conditions at the vent orifice. For this comparison we have used the solubility
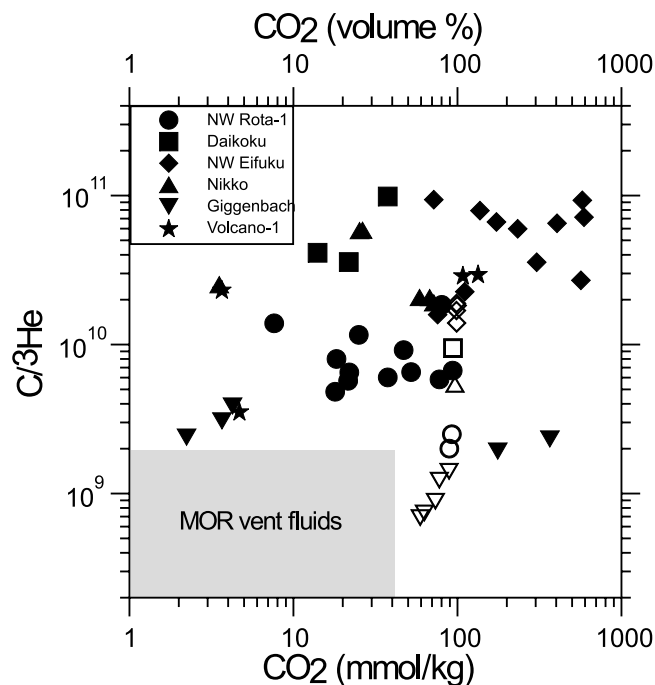

Figure 8. CO$_2$/^{3}He ratio versus CO$_2$ concentration for vent fluids (filled symbols) and gas phase samples (open symbols). For the vent fluids, the scale at the bottom (mmol/kg) applies, while for gas phase samples, the scale at the top (volume %) applies. Note that the majority of the gas phase samples are composed of >90% CO$_2$. The shaded region denotes the region where typical MOR vent fluids would plot.
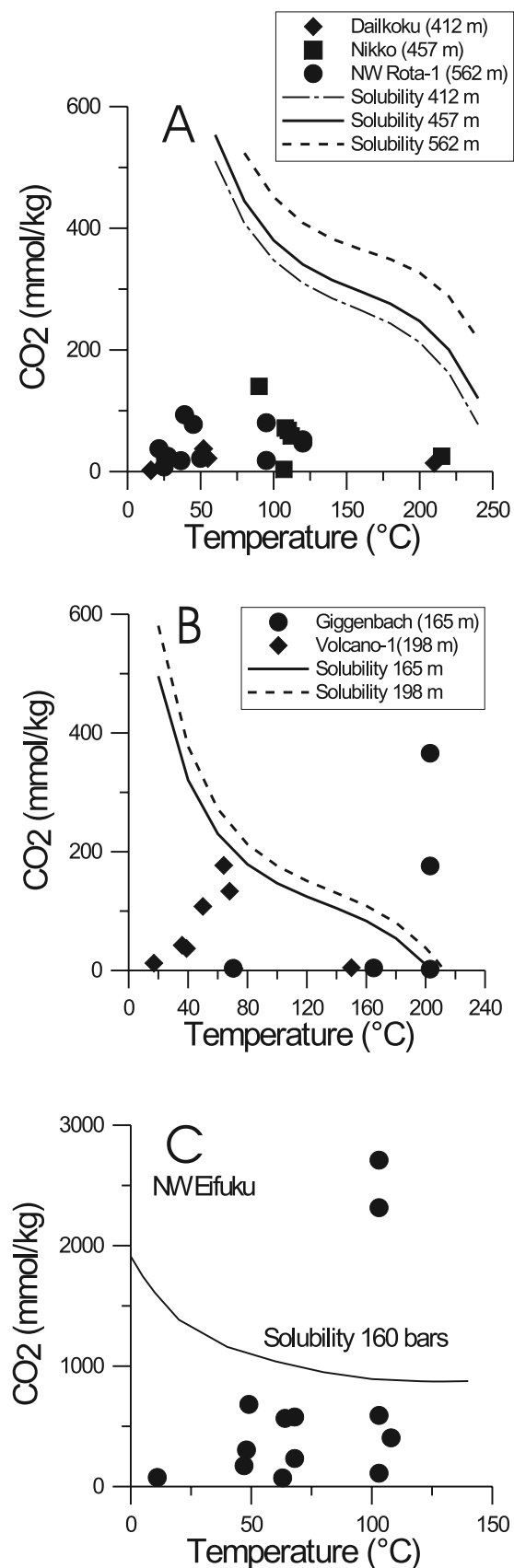
model calculations of *Duan and Sun* [2003] and Z. H. Duan (Thermodynamic properties of the H_2O-CO_2-NaCl system, report, available at http://www.geochem-model.org/models/h2o_co2_nacl2006), using the values for 0.6 m NaCl, equivalent to 35‰ salinity. The CO_2 solubility does decrease with increasing NaCl concentration, although this effect is small compared to the p,T effects. The Z. H. Duan (report, 2006) model agrees extremely well with the original solubility measurements of *Wiebe and Gaddy* [1939].

[27] Figures 9a, 9b, and 9c show vent fluid CO_2 concentrations plotted versus vent temperature. The curves are the corresponding CO_2 solubility curves as calculated using the Z. H. Duan (report, 2006) model. There is a single solubility curve corresponding to the pressure depth of each of the volcanoes. As expected, the solubility goes to zero at the boiling point at that depth. In Figure 9a we were able to combine the vent fluid values and solubility curves for Daikoku, Nikko, and NW Rota-1 in a single plot since the hydrothermal systems on these three volcanoes lie at similar depths. If the CO_2 dissolved in the fluids was in equilibrium with the gas phase, i.e., saturated, then the discrete data points should plot close to the solubility lines. It is immediately apparent that none of the fluid samples collected at these three volcanoes are close to being saturated with CO_2 at the p,T conditions at the vent orifice. Even for the 90°C southern lone vent on Nikko, which has the highest fluid concentration on the plot, the measured CO_2 concentration (140 mmol/kg) is only about 1/3 of the predicted CO_2 solubility of 370 mmol/kg at 90°C, 4.6 bar pressure. A similar condition holds for Volcano-1, although the vent fluid concentrations there approach about 1/2 of the saturation value (Figure 9b).

[28] At Giggenbach a different set of conditions exist. Three of the fluid samples were collected from the Marker 12 vent which was right at the boiling point of 203°C at 165 m depth. Furthermore, as described above in section 4, the venting at Marker 12 consisted of fluid commingled with gas bubbles, making it difficult to collect vent fluid without also trapping some of the gas phase. Two of the 203°C samples collected at Marker 12 have high CO_2 concentrations of 177 and 361 mmol/kg, even though the solubility at that temperature is essentially zero (Figure 9b). We attribute this to incorporation of varying amounts of the pure gas phase into these two fluid samples.

[29] NW Eifuku lies at a much greater depth (1612 m) compared to the other volcanoes discussed here, and the saturation solubility values are correspondingly higher due to the greater pressure (Figure 9c). Furthermore the greater depth results in the CO_2 taking the form of liquid droplets. As discussed by *Lupton et al.* [2006], there was evidence

Figure 9. Vent fluid CO_2 concentration versus vent orifice temperature for (a) Daikoku, Nikko, and NW Rota-1, (b) Giggenbach and Volcano-1, and (c) NW Eifuku. On each plot the saturation solubility curve for CO_2 at the pressure depth of the vent field is shown for comparison. The solubility curves were calculated for CO_2 in 0.6m NaCl solution (equivalent to 35‰ salinity) using the model of *Duan and Sun* [2003] and Z. H. Duan (report, 2006). The Z. H. Duan (report, 2006) model agrees extremely well with the original solubility measurements of *Wiebe and Gaddy* [1939].

that a layer or "pond" of liquid CO_2 was present beneath the surface at the Champagne site, probably capped by a layer of CO_2 hydrate. This is similar to conditions reported at the CO_2-rich site in the Okinawa Trough [*Sakai et al.*, 1990a, 1990b]. The Champagne fluid was venting from short white chimneys at temperatures of ∼100°C, while the liquid CO_2 droplets emerging from the seafloor nearby were cold (<4°C) (Figure 4d). As shown in Figure 9c, the vent fluid CO_2 concentrations at the Champagne site exhibit huge variations from 70 mmol/kg up to 2700 mmol/kg, spanning the solubility value which is about 1000 mmol/kg at this depth. The CO_2 concentration of 2.7 mol/kg is the highest ever reported for deep sea hydrothermal fluids. Although a separate gas phase was not visible in the vent fluid stream, the ascending vent fluid must have penetrated the subsurface layers of liquid CO_2 and CO_2 hydrate before entering the ocean. *Lupton et al.* [2006] attributed the very high and variable CO_2 concentrations at NW Eifuku to entrainment of small amounts of either CO_2 liquid or hydrate into the ascending vent fluid.

7. Discussion and Conclusions

[30] As discussed above, direct submersible investigations were conducted on the active hydrothermal systems of 22 submarine arc volcanoes (11 on the Mariana Arc and 11 on the Tonga-Kermadec Arc). Six of these volcanoes (∼27%) were found to be venting a free gas phase composed mainly of CO_2. In contrast, only one site out of hundreds that have been observed and sampled in the mid-ocean ridge divergent margin setting has shown evidence for a separate gas phase. The high frequency of observed gas venting presented in this work, covering a range of depths, indicates the fundamental importance of magma degassing in hydrothermal systems on volcanic arcs.

[31] Several characteristics of the gases emanating from these six volcanoes point to an origin distinct from that on mid-ocean ridges. First, the concentration of dissolved CO_2 in the vent fluids is an order of magnitude higher than typical vents on MOR systems and is higher than can be achieved by water-rock interaction. Second, the $C/^3He$ ratio is also much higher compared to MOR vents, varying from 3×10^9 up to 1×10^{11} in these six arc volcanoes, compared with $1-2 \times 10^9$ for most MOR systems. Both of these characteristics are due to the higher overall volatile content of magmas in the arc environment, and an excess of carbon dioxide contributed from the subducting slab. The high concentrations of CO_2 and He observed in these volcanic arc hydrothermal systems that vent a free gas phase require the direct injection of magmatic gas into the hydrothermal system. It is not possible to reach concentrations of CO_2 in the aqueous phase above 50 mmol/kg by direct water/rock reaction unless the water/rock ratio is significantly less than one, which is both physically and chemically unreasonable [*Lupton et al.*, 2006]. This suggests that the gas phase in our volcanoes formed separately from the hydrothermal fluid, probably by direct magma chamber degassing.

[32] On the other hand, with the exception of Giggenbach, most of the vent fluids are undersaturated with CO_2, even though a free gas phase is present. At NW Rota-1, Daikoku, Nikko, and Volcano-1, the vent fluid CO_2 concentrations are considerably below the saturation solubility

for CO_2 under the existing p,T conditions. Most of the fluid samples from NW Eifuku are also undersaturated with CO_2 (Figure 9c). However, undersaturation of the CO_2 dissolved in the aqueous phase would not be expected for pressure release degassing of an ascending fluid, since typically 5 to 10% supersaturation is required before bubble nucleation begins [*Li and Yortsos*, 1995; *Frank et al.*, 2007]. Thus one would expect the fluid phase to be slightly supersaturated with CO_2 for the case where the gas phase is forming continuously by degassing of an ascending fluid. The only way undersaturation would occur at the surface is by boiling of the fluid or by mixing and dilution with seawater.

[33] One explanation for the existence of a free gas phase is that dissolved CO_2 has been stripped from the fluid during the separation of a vapor phase, resulting in undersaturation of the fluid. This explanation may apply in boiling systems at low pressure, such as Giggenbach volcano. In this case, shallow boiling of a hydrothermal fluid with relatively high initial CO_2 content can generate a vapor phase that could condense out water with a small degree of cooling and leave a CO_2-rich gas phase. The separate gas and liquid phases could then migrate to the surface, exchanging gas enroute, but not reaching equilibrium, thereby delivering an undersaturated liquid phase, and a gas phase that has a lower $C/^3He$ ratio due to the gas solubility difference. The overall system temperature remains near the boiling point.

[34] A second mechanism to generate a separate CO_2-rich gas phase is direct degassing from a magma chamber. This process was observed directly at NW Rota-1, where CO_2-rich gas bubbles exsolve from slowly erupting lava [*Embley et al.*, 2006; *Chadwick et al.*, 2008]. This process clearly occurs at depth as well as at the seafloor, potentially generating CO_2-rich fluids that can migrate upward. The expression of this gas phase at the seafloor depends on the plumbing system and the temperature profile in the upwelling zone. However, when the CO_2-rich gas phase encounters circulating seawater during ascent through the volcano edifice, a two-phase mixture of CO_2−rich gas and an aqueous phase undersaturated with CO_2 can coexist as buoyant gas bubbles ascend through and exchange with the aqueous phase. This explanation is similar to that proposed by *Lupton et al.* [2006] for NW Eifuku, in which CO_2 directly degasses from a magma chamber, cools while migrating to the seafloor, and eventually forms CO_2 liquid and hydrate near the surface. In this model the 100°C vent fluids at NW Eifuku are created by secondary heating of circulating seawater by the enthalpy carried by the CO_2 gas.

[35] Important questions remain as to why a separate gas phase exists at these six volcanoes, and whether it represents a significant contribution to the oceanic carbon flux. Depth of the hydrothermal site is not a good predictor for the presence of a separate gas phase. With the exception of NW Eifuku, the volcanoes are all relatively shallow (165−560 m), which favors boiling, and the resulting lower solubility of dissolved CO_2 makes it easier for pressure release degassing to occur. However, as shown in Figure 6, the other 16 volcanoes without a free gas phase were also quite shallow and had distinctly lower dissolved CO_2 concentrations compared to those volcanoes with a gas phase. We conclude that the six volcanoes producing a free gas phase are in a state of active magma degassing, and the

remaining 16 hydrothermally active volcanoes are in a different volcanic stage that produces less magmatic gas.

[36] We know very little about the CO_2 flux from these volcanoes. For the Champagne site on NW Eifuku, *Lupton et al.* [2006] estimated the carbon flux at 8×10^8 mol CO_2/a, which is about 0.1% of the global MOR carbon flux. This is remarkable considering that NW Eifuku is a relatively small, young volcano and that the Champagne site itself is quite small in areal extent. Furthermore, at NW Eifuku most of the carbon flux ($\sim$98%) was carried by the liquid CO_2 droplets, with the vent fluid making only a minor contribution. Although liquid CO_2 droplets have a higher carbon concentration than gas bubbles, it still seems likely that most of the carbon flux would be carried by the separate gas phase when it is present as gas bubbles. The presence of a separate gas phase, taken together with the very high concentrations of dissolved CO_2 in the associated vent fluids, suggests that carbon fluxes from the other five volcanoes (NW Rota-1, Daikoku, Nikko, Giggenbach, and Volcano-1) may be equally significant. However, it should be noted that *Hilton et al.* [2002] estimated the carbon flux from an average subaerial arc volcano at 2×10^{10} mol/a, about 25 times higher than the carbon flux from NW Eifuku. Thus the carbon flux at NW Eifuku may be significant in the ocean realm, but not necessarily for the global subaerial carbon flux. The next step should be to conduct detailed experiments to estimate the flux at one or more of these volcanoes in order to assess their contribution to the oceanic carbon inventory.

[37] It is also apparent that all six of these volcanoes may represent valuable natural laboratories for studying the effects of high CO_2 concentrations on marine ecosystems. For example, the effect of CO_2-induced acidity on marine organisms with calcareous shells is already being studied at NW Eifuku, where large mussel beds are in close proximity to the Champagne vent site [*Tunnicliffe et al.*, 2008]. Another site of interest is Volcano-1, where CO_2 gas bubbles are rising directly through a bed of mussels (Figures 4g and 4h). Studies of this type are particularly relevant considering the recent interest in oceanic disposal of fossil fuel CO_2 as a method to alleviate the increase in atmospheric CO_2.

References

Baker, E. T., R. Embley, S. L. Walker, J. A. Resing, J. Lupton, K. Nakamura, C. E. J. de Ronde, and G. Massoth (2008), Hydrothermal activity and volcano distribution along the Mariana arc, *J. Geophys. Res.*, *113*, B08S09, doi:10.1029/2007JB005423.

Baranenko, V. E., L. N. Fal'kovskii, V. S. Kirov, Y. V. Filimonov, Y. E. Lebedev, A. N. Musienko, and A. I. Piontkovskii (1989), Solubility of helium in water, *Atomnaya Energiya*, *66*(5), 354–355.

Butterfield, D. A., G. J. Massoth, R. E. McDuff, J. E. Lupton, and M. D. Lilley (1990), Geochemistry of hydrothermal fluids from Axial Seamount Hydrothermal Emissions Study Vent Field, Juan de Fuca Ridge: Subsea-floor boiling and subsequent fluid-rock interaction, *J. Geophys. Res.*, *95*(B8), 12,895–12,921, doi:10.1029/JB095iB08p12895.

Chadwick, W. W., Jr., D. S. Scheirer, R. W. Embley, and H. P. Johnson (2001), High-resolution bathymetric surveys using scanning sonars: Lava flow morphology, hydrothermal vents and geologic structure at recent eruption sites on the Juan de Fuca Ridge, *J. Geophys. Res.*, *106*(B8), 16,075–16,100, doi:10.1029/2001JB000297.

Chadwick, W. W., Jr., R. W. Embley, C. E. J. De Ronde, R. J. Stern, J. Hein, S. G. Merle, and S. Ristau (2004), The geologic setting of hydrothermal vents at Mariana Arc submarine volcanoes: High-resolution bathymetry and ROV observations, *Eos Trans. AGU*, *85*(47), Fall Meet. Suppl., Abstract V43F-06.

Chadwick, W., K. V. Cashman, R. Embley, H. Matsumoto, R. P. Dziak, C. E. J. de Ronde, T. A. Lau, N. D. Deardorff, and S. G. Merle (2008), Direct video and hydrophone observations of submarine explosive eruptions at NW Rota-1 volcano, Mariana arc, *J. Geophys. Res.*, *113*, B08S10, doi:10.1029/2007JB005215.

de Ronde, C. E. J., E. T. Baker, G. J. Massoth, J. E. Lupton, I. C. Wright, R. A. Feely, and R. R. Greene (2001), Intra-oceanic subduction-related hydrothermal venting, Kermadec forearc, New Zealand, *Earth Planet. Sci. Lett.*, *193*, 359–369, doi:10.1016/S0012-821X(01)00534-9.

de Ronde, C. E. J., et al. (2007), Submarine hydrothermal activity along the mid-Kermadec Arc, New Zealand: Large-scale effects on venting, *Geochem. Geophys. Geosyst.*, *8*, Q07007, doi:10.1029/2006GC001495.

Dixon, J. E. (1997), Degassing of alkalic basalts, *Am. Mineral.*, *82*, 368–378.

Dixon, J. E., D. A. Clague, and E. M. Stolper (1991), Degassing history of water, sulfur, and carbon in submarine lavas from Kilauea volcano, Hawaii, *J. Geol.*, *99*, 371–394.

Duan, Z. H., and R. Sun (2003), An improved model calculating CO_2 solubility in pure water and aqueous NaCl solutions from 273 to 533 K and from 0 to 2000 bar, *Chem. Geol.*, *193*(3–4), 257–271, doi:10.1016/S0009-2541(02)00263-2.

Embley, R. W. (2006), Geological framework for Mariana hydrothermal systems, *Eos Trans. AGU*, *87*(52), Fall Meet. Suppl., Abstract OS34A-01.

Embley, R. W., E. T. Baker, W. W. Chadwick Jr., J. E. Lupton, J. A. Resing, G. J. Massoth, and K. Nakamura (2004), Explorations of Mariana Arc volcanoes reveal new hydrothermal systems, *Eos Trans. AGU*, *85*, 37–40, doi:10.1029/2004EO040001.

Embley, R. W., et al. (2006), Long-term eruptive activity at a submarine arc volcano, *Nature*, *441*, 494–497, doi:10.1038/nature04762.

Embley, R. W., et al. (2007), Exploring the submarine ring of fire–Mariana Arc–western Pacific, *Oceanography*, *20*(4), 68–79.

Frank, X., N. Dietrich, J. Wu, R. Barraud, and H. Z. Li (2007), Bubble nucleation and growth in fluids, *Chem. Eng. Sci.*, *62*, 7090–7097, doi:10.1016/j.ces.2007.08.030.

Gardiner, G. E., and N. O. Smith (1972), Solubility and partial molar properties of helium in water and aqueous sodium chloride from 25 to 100° and 100 to 600 atmospheres, *J. Phys. Chem.*, *76*(8), 1195–1202, doi:10.1021/j100652a019.

Gerth, W. A. (1983), Effects of dissolved electrolytes on the solubility and partial molar volume of helium in water from 50 to 400 atmospheres at 25°C, *J. Sol. Chem.*, *12*(9), 655–669, doi:10.1007/BF00648669.

Hilton, D. R., T. P. Fischer, and B. Marty (2002), Noble gases and volatile recycling at subduction zones, in *Noble Gases in Geochemistry and Cosmochemistry, Rev. Mineral. Geochem.*, vol. 47, edited by D. Porcelli, C. J. Ballentine, and R. Wieler, pp. 319–370, Mineral. Soc. of Am., Washington, D. C.

Hoefs, J. (1980), *Stable Isotope Geochemistry*, 208 pp., Springer, Berlin.

Kelley, D. S., M. D. Lilley, and G. L. Fruh-Green (2004), Volatiles in submarine environments: Food for life, in *The Subseafloor Biosphere at Mid-Ocean Ridges, Geophys. Monogr. Ser.*, vol. 144, edited by W. Wilcock et al., pp. 167–190, AGU, Washington, D. C.

Li, X., and Y. C. Yortsos (1995), Theory of multiple bubble growth in porous media by solute diffusion, *Chem. Eng. Sci.*, *50*(8), 1247–1271, doi:10.1016/0009-2509(95)98839-7.

Lilley, M. D., E. J. Olson, J. E. Lupton, and K. L. Von Damm (1992), Volatiles in the 9°N hydrothermal system: A comparison of 1991 and 1992 data, *Eos Trans. AGU*, *73*(43), Fall Meet. Suppl., 524.

Lupton, J., D. Butterfield, M. Lilley, J. Ishibashi, D. Hey, and L. Evans (1999), Gas chemistry of hydrothermal fluids along the East Pacific Rise, 5°S to 32°S (abstract), *Eos Trans. AGU*, *80*(46), Fall Meet., Suppl., F1099.

Lupton, J., et al. (2006), Submarine venting of liquid carbon dioxide on a Mariana Arc volcano, *Geochem. Geophys. Geosyst.*, *7*, Q08007, doi:10.1029/2005GC001152.

Massoth, G., C. de Ronde, J. Lupton, R. Feely, E. Baker, G. Lebon, and S. Maenner (2003), Chemically rich and diverse submarine hydrothermal plumes of the southern Kermadec volcanic arc (New Zealand), in *Intra-Oceanic Subduction Systems: Tectonic and Magmatic Processes*, edited by R. D. Larter and P. T. Leat, *Geol. Soc. Spec. Publ.*, *219*, 119–139.

Massoth, G., et al. (2007), Multiple hydrothermal sources along the south Tonga arc and Valu Fa Ridge, *Geochem. Geophys. Geosyst.*, *8*, Q11008, doi:10.1029/2007GC001675.

Merle, S., S. Ristau, R. Embley, and W. Chadwick (2004), *Submarine Ring of Fire 2004—Mariana Arc*, 275 pp., NOAA, Silver Spring, Md. (Available at http://oceanexplorer.noaa.gov/explorations/04fire/logs/summary/media/marianas2004cruisereport.pdf)

Merle, S., R. Embley, and A. Malahoff (2005), *Cruise Report for New Zealand American SRoF 2005—Kermadec Arc Submarine Volcanoes*, 275 pp., NOAA, Silver Spring, Md. (Available at http://oceanexplorer.noaa.gov/explorations/05fire/logs/leg2_summary/media/srof05_cruisereport_final.pdf)

Merle, S., R. Embley, and W. Chadwick (2006), *Cruise Report for SRoF 2006–Mariana Arc Submarine Volcanoes*, 242 pp., NOAA, Silver Spring, Md. (Available at http://oceanexplorer.noaa.gov/explorations/06fire/logs/summary/media/srof06_cruisereport_final.pdf)

Nakamura, K. (2005), R/V *Natsushima* NT05–18 Cruise Report, 53 pp., Natl. Inst. of Adv. Ind. Sci. and Technol., Tsukuba, Japan, Nov.

Resing, J. A., J. E. Lupton, R. A. Feely, and M. D. Lilley (2004), CO_2 and ^{3}He in hydrothermal plumes: Implications for mid-ocean ridge CO_2 flux, *Earth Planet. Sci. Lett.*, *226*, 449–464, doi:10.1016/j.epsl.2004.07.028.

Sakai, H., T. Gamo, E.-S. Kim, K. Shitashima, F. Yanagisawa, and M. Tsutsumi (1990a), Unique chemistry of the hydrothermal solution in the Mid-Okinawa Trough backarc basin, *Geophys. Res. Lett.*, *17*, 2133–2136, doi:10.1029/GL017i012p02133.

Sakai, H., T. Gamo, E.-S. Kim, M. Tsutsumi, T. Tanaka, J. Ishibashi, H. Wakita, M. Yamano, and T. Oomori (1990b), Venting of carbon dioxide-rich fluid and hydrate formation in Mid-Okinawa Trough backarc basin, *Science*, *248*, 1093–1096, doi:10.1126/science.248.4959.1093.

Sano, Y., and S. N. Williams (1996), Fluxes of mantle and subducted carbon along convergent plate boundaries, *Geophys. Res. Lett.*, *23*, 2749–2752, doi:10.1029/96GL02260.

Stoffers, P., T. Worthington, U. Schwarz-Schampera, L. Evans, M. Hannington, R. Hekinian, L. Lundsten, G. Massoth, M. Schmidt, and R. Vaiomo'unga (2005), Cruise Report for SITKAP, 112 pp., Inst. für Geowis. Univ. Kiel, Kiel, Germany, June.

Stoffers, P., et al. (2006), Submarine volcanoes and high-temperature hydrothermal venting on the Tonga arc, southwest Pacific, *Geology*, *34*, 453–456, doi:10.1130/G22227.1.

Top, Z., W. C. Eismont, and W. B. Clarke (1987), Helium isotope effect and solubility of helium and neon in distilled water and seawater, *Deep Sea Res.*, *34*(7), 1139–1148, doi:10.1016/0198-0149(87)90068-9.

Tunnicliffe, V., K. T. Davies, D. A. Butterfield, R. W. Embley, and C. Rideout (2008), Calcification of mussel shells in a setting of high carbon dioxide release on a seamount in the Mariana volcanic arc: Biotic responses to a low pH ocean, paper presented at ASLO Ocean Sciences Meeting, Am. Soc. of Limnol. and Oceanogr., Orlando, Fla., March.

van Soest, M. C., D. R. Hilton, and R. Kreulen (1998), Tracing crustal and slab contributions to arc magmatism in the Lesser Antilles island arc using helium and carbon relationships in geothermal fluids, *Geochim. Cosmochim. Acta*, *62*, 3323–3335, doi:10.1016/S0016-7037(98)00241-5.

Von Damm, K. L. (1995), Controls on the chemistry and temporal variability of seafloor hydrothermal fluids, in *Seafloor Hydrothermal Systems: Physical, Chemical, Biological, and Geological Interactions*, *Geophys. Monogr. Ser.*, vol. 91, edited by S. E. Humphris et al., pp. 222–247, AGU, Washington, D. C.

Von Damm, K. L., et al. (1995), Evolution of East Pacific Rise hydrothermal vent fluids following a volcanic eruption, *Nature*, *375*, 47–50, doi:10.1038/375047a0.

Wallace, P. J. (2005), Volatiles in subduction zone magmas: Concentrations and fluxes based on melt inclusion and volcanic gas data, *J. Volcanol. Geotherm. Res.*, *140*, 217–240, doi:10.1016/j.jvolgeores.2004.07.023.

Weiss, R. F. (1970), Helium isotope effect in solution in water and seawater, *Science*, *168*, 247–248, doi:10.1126/science.168.3928.247.

Weiss, R. F. (1971), The solubility of helium and neon in water and seawater, *J. Chem. Eng. Data*, *16*, 235–241, doi:10.1021/je60049a019.

Weiss, R. F. (1974), Carbon dioxide in water and seawater: The solubility of a non-ideal gas, *Mar. Chem.*, *2*, 203–215, doi:10.1016/0304-4203(74)90015-2.

Wiebe, R., and V. L. Gaddy (1935), The solubility of helium in water at 0, 25, 50, and 75° and at pressures to 1000 atmosphere, *J. Am. Chem. Soc.*, *57*, 847–851, doi:10.1021/ja01308a017.

Wiebe, R., and V. L. Gaddy (1939), The solubility in water of carbon dioxide at 50, 75, and 100°, at pressures to 700 atmospheres, *J. Am. Chem. Soc.*, *61*, 315–318, doi:10.1021/ja01871a025.

————————

D. Butterfield, JISAO, University of Washington, 7600 Sand Point Way NE, Seattle, WA 98115-6349, USA.

B. Christenson, Institute of Geological and Nuclear Sciences, P.O. Box 31, Lower Hutt 31-312, New Zealand.

R. Embley and J. Lupton, Pacific Marine Environmental Laboratory, NOAA, 2115 SE OSU Drive, Newport, OR 97365-5258, USA. (john.e.lupton@noaa.gov)

L. Evans, CIMRS, Oregon State University, 2030 Marine Science Drive, Newport, OR 97365-5258, USA.

M. Lilley, School of Oceanography, University of Washington, Seattle, WA 98195, USA.

G. Massoth, Mass-Ex3 Consulting LLC, 2100 Lake Washington Boulevard N, N101, Renton, WA 98056, USA.

K. Nakamura, National Institute of Advanced Science and Technology, Ibaraki, Tsukuba 305-8567, Japan.

M. Schmidt, Institute of Geosciences, University of Kiel, D-24118 Kiel, Germany.